THE JOURNAL

OF THE

AMERICAN CERAMIC SOCIETY

APRIL 1, 1945

MONTHLY PUBLICATION DEVOTED TO THE ARTS AND SCIENCES RELATED TO THE SILICATE INDUSTRIES

TABLE OF CONTENTS

Vol. 28 April 1, 1945 No. 4

Journal of The American Ceramic Society

System Magnesium Oxide–Boric Oxide 97–102
By H. M. Davis and M. A. Knight

Relation of Metal Thickness, Enamel Thickness, and Bottom Radius to Impact Resistance of Porcelain Enameled Utensils 102–109
By F. A. Petersen and A. I. Andrews

Fundamental Properties of Raw Clays Influencing Their Use 110–18
By C. G. Harman and C. W. Parmelee

Splitting Soft-Mud Brick 118–20
By H. G. Schurecht and J. F. McMahon

Publication Office: 20th & Northampton Sts., Easton, Pa.
Editorial Office: 2525 N. High St., Columbus 2, Ohio
Committee on Publications: R. L. Stone, *Chairman;* R. E. Birch, H. Z. Schofield, H. Thiemecke, and R. C. Purdy, *ex officio*

Entered as second-class matter at the post office at Easton, Pa., under the act of March 3, 1879. Published monthly
Subscription fifteen dollars ($15.00) a year. Single numbers $1.50
(*Foreign and Canadian postage, 50c additional on subscriptions*)
(*Copyright 1945, American Ceramic Society, Inc.*)

THE JOURNAL
OF
THE AMERICAN CERAMIC SOCIETY

Vol. 28 April 1, 1945 No. 4

THE SYSTEM MAGNESIUM OXIDE–BORIC OXIDE*

By H. M. Davis† and M. A. Knight‡

Abstract

Equilibrium in the system has been investigated for compositions from 0.6 to 75 weight per cent MgO. Three intermediate compounds are present. $MgO \cdot B_2O_3$ melts incongruently at 988°C. to form $2MgO \cdot B_2O_3$ and a liquid containing more than 99% B_2O_3. The other two compounds melt congruently: $2MgO \cdot B_2O_3$ at 1340°C. and $3MgO \cdot B_2O_3$ at 1366°C. At 1142°C., a region of liquid immiscibility extends from 0.6 to 36.0% MgO. Temperatures are accurate within ±5°C. Conflicts between these results and those of Toropov and Konovalov (see footnote 8) are discussed.

I. Introduction

The well-known use of boric oxide as a mineralizer has been applied to magnesia and magnesia-containing bodies in ceramic processes. An understanding of the reactions of boric oxide with magnesium oxide has a direct bearing on applications of this type. The object of this research has been the determination of the phase equilibria in the system magnesium oxide–boric oxide, subject to the limitation imposed by platinum ware. Information on this system will contribute to the accumulating data on phase equilibria in mixtures of oxides having ceramic and petrologic significance.

II. Previous Work

Kracek, Morey, and Merwin[1] have reported that the melting point of B_2O_3 is 450 ± 2° §. Working with small crystals, they found the crystals nearly or quite uniaxial, with ω (or β and γ) = 1.64$_8$, and ϵ (or α) = 1.61$_5$. Crushing either induces a minute lamellar twinning or reveals a twinning caused by inversion. Kanolt[2] found 2800° as the melting point of MgO in a nitrogen atmosphere. Winchell[3] reports the properties of MgO formed from fusion as: isometric in cubes, octahedrons, and grains with perfect 100 cleavage and imperfect 111 cleavage; crystals with the NaCl space lattice; colorless; and isotropic with n = 1.734–1.737.

Only the orthoborate, $3MgO \cdot B_2O_3$, has been reported as a natural mineral, the "Kotoite" of Watanabe.[4] Its properties are similar to those of the orthoborate formed in laboratory fusions.

In the studies of the solubility of alkaline earth oxides in boric oxide, a variety of compounds was listed in early works. Of these, only the metaborate ($MgO \cdot B_2O_3$), pyroborate ($2MgO \cdot B_2O_3$), and orthoborate ($3MgO \cdot B_2O_3$) have been confirmed in later work, and there has been considerable controversy over the existence of the equimolar compound. LeChatelier[5] confirmed the pyro- and the ortho-borate. Guertler[6] found that two liquids formed when MgO and B_2O_3 were melted together. When cooled and isolated, the heavier, MgO-rich liquid was found to contain 34.45%* MgO and to consist of crystals of $2MgO \cdot B_2O_3$ in borate-rich glass. He also confirmed $3MgO \cdot B_2O_3$ but found

---

* Presented at the Forty-Fifth Annual Meeting, The American Ceramic Society, Pittsburgh, Pa., April 21, 1943 (Refractories Division). Received February 6, 1945.

Taken in part from a thesis presented by the junior author in partial fulfillment of the requirements for the degree of Doctor of Philosophy at The Pennsylvania State College, August, 1942.

† Assistant Professor of Metallurgy, The Pennsylvania State College, State College, Pa.

‡ Research Associate, Preston Laboratories, Butler, Pa., formerly Graduate Fellow, Department of Ceramics, The Pennsylvania State College, State College, Pa.

§ All temperatures are in degrees Centigrade.

[1] F. C. Kracek, G. W. Morey, and H. E. Merwin, "The System Water–Boron Oxide," *Amer. Jour. Sci.*, **35**, 143–71 (1938); abstracted from *Jour. Wash. Acad. Sci.* in *Ceram. Abs.*, **18** [2] 61 (1939).

[2] C. W. Kanolt, "Melting Points of Some Refractory Oxides," *Jour. Wash. Acad. Sci.*, **3** [11] 315–18 (1913).

[3] A. N. Winchell, Microscopic Characters of Artificial Minerals, 2d ed., pp. 99, 116. John Wiley and Sons, Inc., New York, 1931; *Ceram. Abs.*, **11** [5] 323 (1932).

[4] T. Watanabe, "Kotoite, a New Rock-Forming Magnesium Borate," *Mineralog. & Petrog. Mitt.*, **50**, 441–62 (1939); *Ceram. Abs.*, **19** [3] 75 (1940).

[5] H. LeChatelier, "On the Metallic Borates," *Compt. rend.*, **113**, 1034–36 (1891).

[6] W. Guertler, "On the Limits of Miscibility of Boric Oxide and Borates in Melts," *Z. Anorg. Chem.*, **40**, 225–53 (1904); "On the Melting Points of Mixtures of Alkaline Earths with Boric Oxide," *ibid.*, pp. 337–54.

* All compositions are in weight per cent.

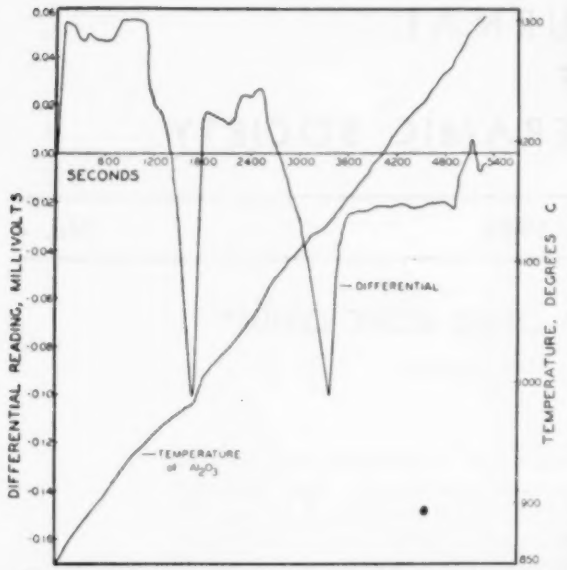

FIG. 1.—Heating curve obtained on charge containing 43.8% MgO. The three endothermic effects at approximately 1800, 3400, and 4900 seconds are, respectively, the incongruent melting of $MgO \cdot B_2O_3$ at 988°C.; the reaction at 1142° between liquid (*a*) and $2MgO \cdot B_2O_3$ to give liquid (*b*); and the end of melting of residual $2MgO \cdot B_2O_3$ at the liquidus.

FIG. 2.—Photomicrograph of small crystals of $MgO \cdot B_2O_3$ (970 ×). Plane polarized light.

no other compounds. The immiscibility of MgO and B_2O_3 was also recorded by Foëx,[7] who gave the MgO-contents of the heavy and the light liquids as 34.15 and 0.63%, respectively. The latest published work on these compounds is that of Toropov and Konovalov,[8] whose analyses yield 0.8 to 36.3% MgO as the extent of the region of liquid immiscibility. Their results are discussed in section V (3).

III. Experimental Methods

In the present study, each batch was prepared from chemically pure boric acid and magnesium basic carbonate. The boric acid was first strongly ignited at about 1300° in a platinum crucible. On the basis of the weight of this B_2O_3 glass, the desired amount of the basic carbonate was dissolved in the glass, and the batch was then ignited for half an hour at temperatures well above its liquidus temperature. After being ground in an agate mortar to pass a 100-mesh screen, the charge was again ignited and then again powdered. At the temperatures of the ignitions, the high fluidity of the charges allowed the ready attainment of homogeneity.

Each batch was analyzed volumetrically for both MgO and B_2O_3. The MgO was determined by solution in standard sulfuric acid, followed by the titration (methyl orange) of the excess acid with standard sodium hydroxide solution. On these same samples, the B_2O_3 was then fortified with neutral invert sugar solution and was titrated with the standard base to the phenolphthalein end point.

The thermal analyses were carried out by standard heating-curve and quenching techniques in a cascade-type, platinum resistance furnace with a secondary winding of Kanthal-A resistance wire. Because of the high rate of crystallization of all melts containing more than 0.6% MgO, the quenching method was used only in the preparation of equilibrium phases for petrographic and X-ray diffraction studies. A regulator responding to 0.5° temperature change in the furnace was used in the constant-temperature work in conjunction with a Pt, Pt-Rh thermocouple. Heating curves were used to determine the liquidus and inversion temperatures, with several check runs on each batch. A three-lead differential thermocouple was used with a two-compartment platinum crucible, the reference material being freshly calcined pure Al_2O_3. A reproducibility of ±3° was realized in these measurements. Figure 1 shows a typical heating curve obtained on a charge (43.8% MgO) of composition between those of the metaborate and pyroborate compounds.

All thermocouples were checked against a standard thermocouple* and against the melting points of potassium sulfate, 1069° (Roberts[9]), and of calcium orthoborate, 1298° (Carlson[10]), at intervals throughout the work. Since the uncertainty ascribed to the

[7] M. Foëx, "Contribution to Study of Solubilities and Partitions in Glasses," *Ann. Chim.*, **11**, 359–452 (1939); specifically pp. 375–80 on solubilities of oxides in boric anhydride; *Ceram. Abs.*, **19** [11] 255 (1940).

[8] N. A. Toropov and P. F. Konovalov, "Binary System Magnesium Oxide–Boron Anhydride" (in Russian), *Zhur. Fiz. Khim.* (U.S.S.R.), **14**, 1103–1109 (1940); *Chem. Abs.*, **35**, 3886; *Ceram. Abs.*, **20** [6] 157 (1941).

* Pt, Pt-Rh thermocouple, National Bureau of Standards No. 5572, had no considerable deviations at the Bureau from the standard millivoltages.

[9] H. S. Roberts, "Some New Standard Melting Points at High Temperatures," *Phys. Rev.*, **23**, 386–95 (1924); *Ceram. Abs.*, **3** [8] 252–53 (1924).

[10] E. T. Carlson, "The System $CaO–B_2O_3$," *Jour. Research Nat. Bur. Standards*, **9**, 825–32 (1932); RP 510.

TABLE I

PROPERTIES OF BINARY COMPOUNDS

Properties	Metaborate ($MgO \cdot B_2O_3$)	Pyroborate ($2MgO \cdot B_2O_3$)	Orthoborate ($3MgO \cdot B_2O_3$)
Melting point (°C.)	988 ± 5, incongruent	1340 ± 5, congruent	1366 ± 5, congruent
Optical character	Biaxial (−)*	Biaxial (−)	Biaxial (+)†
Crystal system		Monoclinic or triclinic	Orthorhombic
2V	Large*	Approx. 40°	21 ± 1°
Indices of refraction	Min. 1.605	α = 1.589	α = 1.6527
	Max. 1.660	β = 1.660	β = 1.6537
		γ = 1.674	γ = 1.6748
Cleavage		Perfect, perpendicular to acute bisectrix	Good 100
Crystal form	Prismatic with negative elongation	Platy fragments	Prismatic

* After Toropov and Konovalov.[8]
† Remainder of column after Winchell.[3]

TABLE II

HEATING CURVE RESULTS

Run No. (1)	MgO (wt.%) (2)	Endothermic effects at °C.* (3)	(4)	(5)
26	16.4	990	1143	
27	"		1143	
21	25.9	994	1143	
23	"	989	1148	
24	"	992	1142	
53	31.0	990	1138	
54	"		1147	
55	"		1139	
18	34.4	990	1142	
19	"		1143	
20	"	987	1143	
28	36.0	986	1142	
4	36.8	985	1142	
40	39.6	985	1140	(†)
41	"	985	1139	(†)
67	"	988	1142	1219
56	42.5	986	1135	1266
57	"		1144	1275
58	"	987	1138	1272
59	"		1139	1268
61	"	989	(†)	(†)
62	46.4	985	1126	1303
63	"	986	1136	1313
49	47.8	983	1126	1308
50	"	983	1125	1308
51	"		1144	1309
52	"	984	1142	1309
37	53.2	(‡)	(‡)	1337
38	"	(‡)	(‡)	1337
39	"	(‡)	(‡)	1338
73	53.8	(‡)	(‡)	1339
74	"	(‡)	(‡)	1340
75	55.4	1311	1334	
76	"	1312	1334	
77	"	1326	1333	
85	56.3	1315	1330	
86	"	1322	1325	
78	58.8	1313	1326	
79	"		1326	
80	60.5	1311	1344	
81	"	1313	1341	
82	"	1319	1349	
83	62.6	1305	1339	
84	"	1314	1361	
87	67.0	1357	1364	
88	"	1357		
89	"	1353	1363	
90	"		1369	
91	"		1361	
92	"		1362	
96	71.5	1360		
105	"	1359		
106	"	1359		
98	73.5	1358		
99	"	1360		
100	"	1359		
107	"	1359		
101	76.0	1357		
102	"	1360		
104	"	1361		
109	"	1359		

* Endothermic reactions causing respective effects.

Column	Reaction	Range (wt.% MgO)
(3)	$MB \rightleftharpoons M_2B$ + liquid (a)	Up to 53.66
(4)	M_2B + liquid (a) $\rightleftharpoons$ {two liquids or liquid (b) + M_2B}	Up to 53.66
(5)	M_2B + liquid (b) $\rightleftharpoons$ liquid	36.67– 57.7
(6)	(Eutectic) $M_2B + M_3B \rightleftharpoons$ {M_2B + liquid or M_3B + liquid}	53.66– 63.46
(7)	{M_2B + liquid or M_3B + liquid} $\rightleftharpoons$ liquid	53.66– 63.46
(8)	(Eutectic) $M_3B + MgO \rightleftharpoons$ {M_3B + liquid or MgO + liquid}	63.46–100.00
(9)	{M_3B + liquid or MgO + liquid} $\rightleftharpoons$ liquid	63.46–100.00

† Temperature range of run did not include this effect.
‡ No noticeable effect is to be expected this near to compound M_2B.

standard thermocouple used for the checking was ±2°, the maximum error in the temperatures is considered to be within ±5°.

The phases were examined with the petrographic microscope. *X*-ray diffraction patterns were made on certain samples, using copper K radiation and a large-radius powder camera with dual slits for simultaneous exposure of two samples.

IV. Experimental Results

(1) Binary Compounds

The properties of the three binary compounds present in the system are listed in Table I.

(*A*) *Magnesium Metaborate*, $MgO \cdot B_2O_3$: This compound melts incongruently at 988° to form $2MgO \cdot B_2O_3$ and a liquid containing more than 99% B_2O_3 (see section V). Because of the high viscosity and relatively small amount of the liquid in equilibrium with it, this compound does not crystallize readily, and only very small crystals of it were obtained (see Fig. 2). These crystals were biaxial and showed oblique extinction. They were prismatic in habit and showed negative elongation. Indices of refraction found for the crystals as they lay with their principal elongation directions in the plane of the microscope stage were: maximum, 1.660; minimum, 1.605. The larger crystals (Fig. 2)

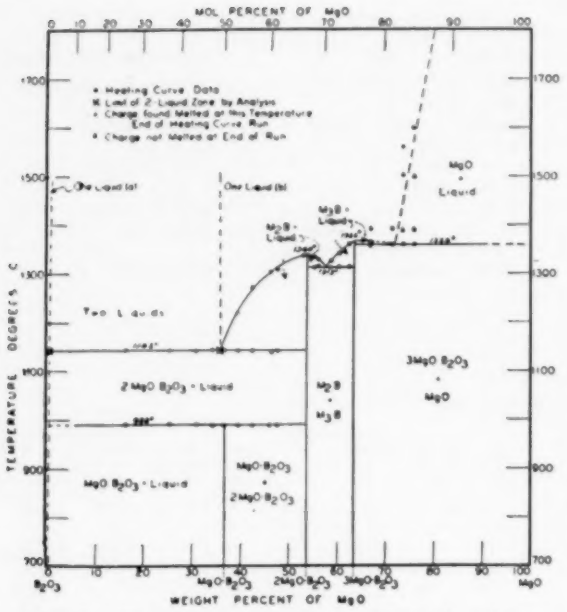

FIG. 3.—The system magnesium oxide–boric oxide.

showed definite development of two faces on either end at angles of 52° and 124° to the elongation.

(*B*) *Magnesium Pyroborate*, $2MgO \cdot B_2O_3$: The pyroborate has a congruent melting point at 1340°. A pronounced cleavage perpendicular to the acute bisectrix causes a predominance of clear, platy crystal fragments, with certain crystals giving traces of two cleavages at an angle of about 50 degrees to each other. The inclined extinction shown in these crystals indicates their being in either the monoclinic or triclinic system. In crystals quenched from immiscible melts, there appears to be some tendency toward twinning.

The crystals are biaxial negative, show high double refraction, and have a 2V of approximately 40°; N_α = 1.589; N_β = 1.660; N_γ = 1.674.

(*C*) *Magnesium Orthoborate*, $3MgO \cdot B_2O_3$: This compound melts congruently at 1366°. In general appearance, its crystals resemble those of the pyroborate. The optical properties of the crystals obtained in the present work agree with those given in the literature; see section I and Table I.

(2) Phase Equilibrium Diagram

The phase equilibrium diagram shown in Fig. 3 was derived from (*a*) the heating-curve analyses listed in Table II and (*b*) petrographic and X-ray studies of constant-temperature preparations.

The liquidus curve has been established from 0.6 to 75% MgO. Between 0.0 and 0.6% MgO, the liquidus rises very rapidly to 1142°. This narrow zone must include the peritectic point at 988°, the temperature of the dissociation of $MgO \cdot B_2O_3$. The two-liquid region at 1142° was found to extend from 0.6 to 36.0% MgO. Table III shows the results of chemical analyses of the mechanically separated layers of charges quenched from just above this liquidus.

TABLE III
ANALYSES OF IMMISCIBLE PHASES

MgO-rich phase (wt.%)		B_2O_3-rich phase (wt.%)	
MgO	B_2O_3	MgO	B_2O_3
			99.4
36.0	64.0	0.6	99.4
35.4	64.6	0.7	99.3
35.8	64.2	0.4	99.6
37.0	63.0	0.6	99.4
Avg. 36.0	64.0	0.6	99.4

To the MgO side of the immiscibility gap, the liquidus consists of simple eutectic forms. From the 36.0% point, the liquidus rises to 1340° and the melting point of the pyroborate, at 53.66% MgO. The eutectic between the pyroborate and the orthoborate falls at 57.7% MgO and 1313°, and the eutectic between the orthoborate and MgO is at 1358°, which is only 8° below the melting point, at 1366°, of $3MgO \cdot B_2O_3$ (63.46% MgO). In samples richer in MgO than 68%, only the eutectic thermal effect was found in the heating curves. From 68% to the eutectic composition, the minor effect due to the final melting was masked by the eutectic break. To the MgO side of the eutectic, the effect of the melting of the last, small amount of solid at the very steep liquidus was too slight to be definitely determined. The location of this liquidus, which rises sharply from the eutectic to the melting point of MgO at 2800°, is somewhat uncertain. Its determination was limited to observation of the melted or unmelted nature of the charges after runs ending at various temperatures. This procedure placed the eutectic at 72% MgO.

V. Discussion of Results

(1) Stability Range of the Metaborate

Much uncertainty has existed concerning the metaborate. Its thermal behavior was particularly obscure and therefore has received especial attention in the present study. As stated in section IV, the compound melts incongruently at 988°. That statement is supported by the following argument.

In all batches having compositions between 0.6% MgO and the compound $2MgO \cdot B_2O_3$ (53.66% MgO), charges quenched after several hours at temperatures between 988° and 1142° showed the pyroborate as the single stable crystalline phase. In the same composition range, charges quenched from below 988° contained the metaborate as a stable crystalline phase; but if the batch composition lay between $MgO \cdot B_2O_3$ and $2MgO \cdot B_2O_3$, both of these compounds were present. When quenched from 950°, charges richer in B_2O_3 than $MgO \cdot B_2O_3$ gave the equimolar compound as the only stable crystalline phase; presumably, this relationship obtains at lower temperatures until crystalline B_2O_3 becomes an equilibrium phase.

(2) X-Ray Diffraction Studies

The above results were obtained through X-ray and petrographic examination of charges quenched from the designated regions. In Table IV are listed the properties of the samples on which the X-ray diffraction patterns shown in Fig. 4 were obtained (powder

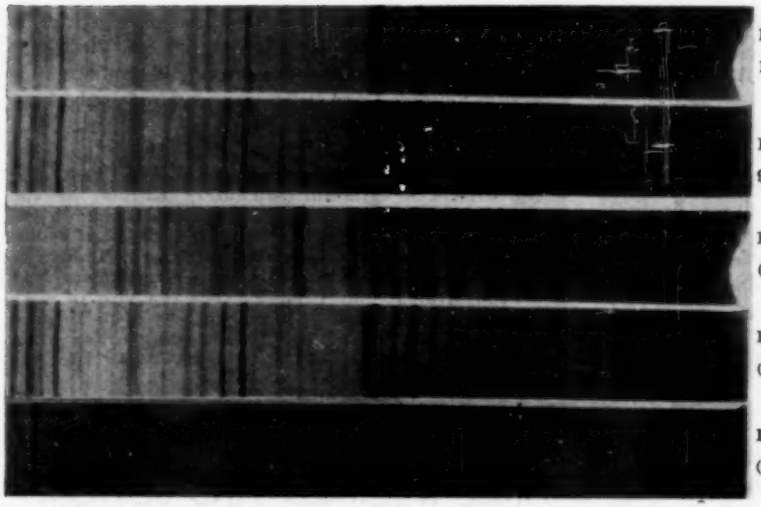

FIG. 4.—X-ray diffraction patterns obtained simultaneously on samples B23 and B24, with reference patterns of the three compounds from batches 18, 30, and 38. The sample B24, quenched from 950°C., exhibits the characteristic patterns of both $MgO \cdot B_2O_3$ and $2MgO \cdot B_2O_3$, whereas B23, quenched from 1075°, shows only the $2MgO \cdot B_2O_3$.

TABLE IV

SAMPLES USED IN X-RAY STUDIES (SEE FIG. 4)

No.	Name	% MgO	Heat-treatment	Equilibrium phases
1	B23 1075	40.0	2 hr. at 1075°; air quenched	$2MgO \cdot B_2O_3$ + liquid
2	B24 950	47.0	12 hr. at 950°; air quenched	$MgO \cdot B_2O_3 + 2MgO \cdot B_2O_3$
3	B18 (1:1)	25.0	12 hr. at 950°; air quenched	$MgO \cdot B_2O_3$ + liquid
4	B30 (2:1)	54.0	Cooled from melt	$2MgO \cdot B_2O_3$
5	B38 (3:1)	68.5	Cooled from melt	87% $3MgO \cdot B_2O_3$ + 13% MgO

method). An examination of the lines in these patterns conclusively reveals the definite differentiation of the three binary compounds and the consistency of the present diagram (Fig. 3) with the phases comprising the various samples. Both macroscopic and microscopic examination of these and other charges substantiated these conclusions.

(3) Work of Toropov and Konovalov

To facilitate comparison, the diagram obtained by Toropov and Konovalov is shown herewith in Fig. 5.

The principal differences between their results and those of the present work are the discrepancies in the temperature of the liquidus curves and in the behavior of the metaborate.

In the Russian paper, Toropov and Konovalov make no mention of any check or calibration of their pyrometric devices. Their temperatures differ from those reported here by variable amounts, the divergence attaining a maximum of 46°. Except where they fixed liquidus temperatures by means of cooling curves (subject to undercooling), their temperatures are higher. In all charges richer in MgO than $2MgO \cdot B_2O_3$, they report a superposition of the eutectic and final melting effects in the heating curves. This is in contrast to the present work, where distinct effects were found up to 68% MgO. For the eutectic temperatures, they chose the start of the break on cooling curves, in which curves they found large undercooling. The present authors found that large and variable undercooling effects made cooling curves unreliable. Especially great effects were observed in this work near the $2MgO \cdot B_2O_3$–$3MgO \cdot B_2O_3$ eutectic, where a pronounced recalescence took place after extreme undercooling. For the temperatures of final melting, the Russian authors used the maxima in the breaks in heating curves.

They report a low-temperature exothermic break, 780°, occurring during only the first heating curve on each charge poorer in MgO than $MgO \cdot B_2O_3$ (36.67% MgO). They offer no discussion of this effect. No such effect was observed in the present study, and no explanation for such a break seems apparent.

The source of their endothermic effect shown at 1020° was not discussed by Toropov and Konovalov. An enantiomorphic inversion in the metaborate could cause such an effect. In the present work, however, $2MgO \cdot B_2O_3$ was found by X-ray and petrographic methods to be the stable phase between 988° and the liquidus in this composition range (as is discussed above). Moreover, no change in the temperature of the endothermic break at 1142° was found at the $MgO \cdot B_2O_3$ composition by the present authors.

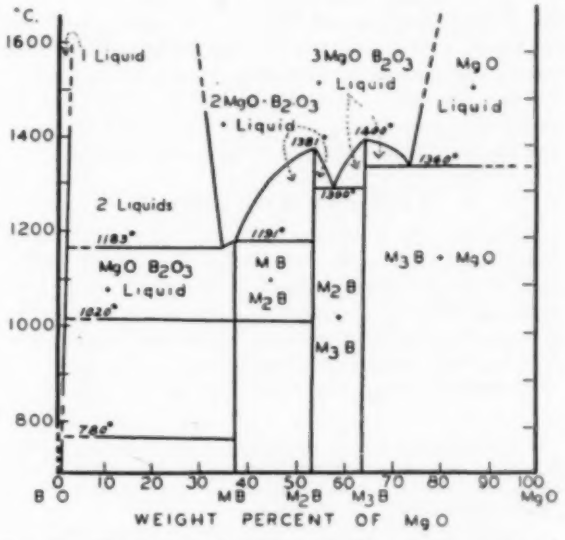

FIG. 5.—The phase diagram according to Toropov and Konovalov (redrawn).

The value of 72.5% MgO recorded by Toropov and Konovalov for the eutectic between $3MgO \cdot B_2O_3$ and MgO agrees quite well with the extrapolated value found in this research.

VI. Summary

Compositions from 0.6 to 75% of MgO have been investigated by means of chemical analyses, heating-curve and quenching tests, and petrographic and X-ray studies. The liquidus and solidus curves have been very nearly completed. The melting behavior of each of the three binary compounds has been established: $MgO \cdot B_2O_3$ melts incongruently at 988°C.; $2MgO \cdot B_2O_3$ melts congruently at 1340°C.; and $3MgO \cdot B_2O_3$ melts congruently at 1366°C. Temperatures are considered correct within ±5°C.

With these data, a phase equilibrium diagram is presented. Certain optical properties of the three intermediate constituents also are reported.

Results obtained are critically compared with those of Toropov and Konovalov.[5]

Acknowledgment

The writers are grateful to Paul D. Krynine of The Pennsylvania State College for the translation of the paper by Toropov and Konovalov. For financial assistance, acknowledgment is made to the Mineral Industries Experiment Station and to the Council on Research of The Pennsylvania State College. The last year of work was made possible through the granting of an Edward Orton, Jr., Ceramic Foundation Fellowship to the junior author.

School of Mineral Industries
The Pennsylvania State College
State College, Pennsylvania

RELATION OF METAL THICKNESS, ENAMEL THICKNESS, AND BOTTOM RADIUS TO IMPACT RESISTANCE OF PORCELAIN ENAMELED UTENSILS *

By F. A. Petersen and A. I. Andrews

Abstract

Three series of standard two-quart pudding pans of different metal thicknesses, coated with one, two, and three coats, respectively, of enamel were tested for impact resistance, using the Enameled Utensil Manufacturers' Council standard impact test. The impact resistance of the pans was increased with increase (1) in metal thickness of the pans, (2) of the enamel thickness, and (3) in the size of the bottom radius. The size of the chip formed on impact also increased with increase in enamel thickness.

The literature dealing with the fracture of glass and enamels is reviewed, and the factors influencing spontaneous chipping and chipping caused by bending and impact are discussed.

I. Introduction

One of the most frequently discussed problems of the porcelain enamel industry is that of chipping although it is not generally understood. In an effort to clarify the general conception of this type of failure, the different causes of chipping and the factors influencing these causes are analyzed. Chipping caused by impact on the bottom radius of enamel pans has been investigated, and the effects of enamel and metal thickness and the size of the radius have been determined.

II. Review of the Literature

Although the literature contains many statements concerning the factors influencing the impact resistance of enameled ware, much uncertainty remains because of conflicting opinions. This lack of conformity is probably a result of different approaches to the problem, insufficient data, and uncontrolled variables.

Several investigators[1] state that an increase in the metal thickness of enamelware increases the durability of the ware. These results are supplemented in data

* Presented at the Forty-Sixth Annual Meeting, The American Ceramic Society, Pittsburgh, Pa., April 4, 1944 (Enamel Division). Received August 24, 1944; revised copy received January 19, 1945.

[1] (*a*) Edward Orton, Jr., "Notes on Testing of Enameled Sheet-Steel Ware," *Trans. Amer. Ceram. Soc.*, **11**, 320–41 (1909)

(*b*) J. B. Shaw, "Testing Sheet-Steel Enamels," *ibid.*, **12**, 463–93 (1910).

(*c*) J. B. Shaw, "Enamel for Sheet Iron and Sheet Steel," *Bur. Standards Tech. Paper*, No. 165, 88 pp., July 22, 1920; p. 74.

(*d*) R. H. Turk, "Comparison of Results Obtained with Impact Machine," *Jour. Amer. Ceram. Soc.*, **13** [11] 887–93 (1930).

(*e*) H. H. Holscher, "Vitreous Enamel Impact Machine," *ibid.*, **15** [6] 353–57 (1932).

(*f*) E. H. Shands, R. H. Turk, and H. G. Wolfram, "Factors Causing Variation of Results in Tests for Physical Properties of Enamels," *ibid.*, **15** [8] 438–43 (1932).

(*g*) E. P. Poste, G. L. Clark, A. I. Andrews, B. T. Sweely, and Mahlon Manson, "Practical and Technical Problems in Enameling," *Ceram. Ind.*, **22** [2] 76–78 (1934); Enamel Bibliography, 1944 ed., p. 220.

(*h*) E. P. Poste, "What 1934 Has Contributed to the Vitreous Enameling Industry," *Ceram. Ind.*, **24** [4] 230–34 (1935); p. 232; for abstract see E. P. Poste, "Porcelain Enamel Industry in 1934, I," Enamel Bibliography, 1944 ed., p. 219.

(*i*) H. H. Holscher, "Relation Between Chipping and Porcelain Enamel Coatings," *Ceram. Ind.*, **24** [6] 348–49 (1935); Enamel Bibliography, 1944 ed., p. 123.

(*j*) Richard Aldinger, "Specifications for Enameled Cooking Vessels," *Keram. Rundschau*, **43** [41] 481–83; [42] 498 (1935); Enamel Bibliography, 1944 ed., p. 7.

(*k*) George Sirovy and E. P. Czolgos, "Enamel Chip-

reported by Andrews and Dietterle,[2] who show that as the metal thickness is increased the force necessary to reach the yield point is also increased.

The effect of enamel thickness on impact resistance specifically has been reported by several writers. Smith,[3] Holscher,[1(e),4] Shands, Turk, and Wolfram,[1(f)] and Turk[1(d)] state that impact resistance decreases with increased enamel thickness. Shands[1(f)] found that with very heavy coatings, 108 gm. per sq. ft. or more, there was an increase of impact resistance after a steady decrease up to that point. Fellows,[5] testing for impact resistance on a radius, reported that the impact resistance increased with enamel thickness. Other writers[6] have stated that, with increased enamel thickness, the degree of deflection of the enameled specimen before fracture occurred was decreased. Andrews and Dietterle[2] and Dietterle[7] showed that an increase of enamel thickness increased the resistance of the enameled test piece to fracture but that the degree of deformation before chipping occurs was decreased. This statement verifies data reported on cross-bend tests. It must be kept in mind, however, that the stress necessary to cause the chipping is much greater with increase of enamel thickness, and therefore the resistance to deformation, whether in bending or impact, increases with increase of enamel thickness. Gehlhoff and Thomas[8] and Murgatroyd[9] report data on impact tests made on glass bulbs and glass bottles showing that the impact resistance increases with increased thickness of the glass at the point of impact.

Another physical property of enamels that affects resistance to impact and chipping is the coefficient of expansion of the ground-coat and cover-coat enamels. Fellows and Wheeler[10] state that decreased expansion of the ground-coat enamel and increased expansion of the cover-coat enamel increased the resistance to impact. Gautsch[11] concludes that decreased expansion in the cover-coat enamel gives an enamel that is more resistant to failure in bending and less resistant to chipping. Aldinger[12] states that cover-coat enamels with a low coefficient of expansion will decrease resistance to chipping. Wolfram and Harrison[13] believe that the coefficient of expansion has varying effects on the resistance of enamel to chipping, depending on the cause of the chipping. In the case of impact failure on a curved surface, they state that an increase in expansion increases the resistance to failure. On a flat surface where the panel is free to deflect, a decrease in the expansion coefficient of the enamel increases the resistance to impact failures. Kinzie and Commons[14] say that if the coefficient of expansion of the enamel is lower than that of the iron, it will probably chip unless other physical properties influenced by composition counteract the effect, whereas an enamel with an expansion higher than that of the iron will probably show less tendency to chip.

Wolff[15] states that improper design of a refrigerator lining causes spontaneous chipping. Aldinger[12(b)]

---

ping, Relation of Ground-Coat Adherence to Thickness and Yield Value of Sheet Steel," *Bull. Amer. Ceram. Soc.*, **17** [4] 168–70 (1938).

(*l*) "You Can Reduce Losses from Damage Due to Chipping of Enamel," *Ceram. Ind.*, **37** [3] 44, 46, 48 (1941); see "Reduction. . .," *Ceram. Abs.*, **21** [1] 6 (1942).

(*m*) E. P. Poste, "Utilization of Porcelain Enamel: II, Sheet-Metal Parts," *Machine Design*, **13** [11] 62–65, 126, 128 (1941); *Ceram. Abs.*, **21** [3] 58 (1942).

(*n*) Arnold E. Barager, "Review of Metal Utensils for Surface Cookery," *Enamelist*, **19** [7] 7–10, 51–54 (April, 1942); reprinted from *Jour. Home Economics*, **33** [10] (December, 1941).

(*o*) "Chipproof Enamelware," *Enamelist*, **10** [4] 22 (1933); Enamel Bibliography, 1944 ed., p. 47.

[2] A. I. Andrews and E. W. Dietterle, "Effect of Enamel on Strength of Enameling Iron," *Jour. Amer. Ceram. Soc.*, **23** [1] 29–32 (1940).

[3] (*a*) P. L. Smith, "Chipping Resistance of Enamels," *Proc. Porcelain Enamel Inst. Forum, Third Forum, Oct., 1938*, pp. 37–47; Enamel Bibliography, 1944 ed., p. 253.

(*b*) P. L. Smith, "Measuring Chipping Resistance of Enamels," *Proc. Porcelain Enamel Inst. Forum, Fourth Forum, Oct., 1939*, pp. 155–60; Enamel Bibliography, 1944 ed., p. 253.

(*c*) P. L. Smith, "Development of Two Tentative Standard Tests," *Proc. Porcelain Enamel Inst. Forum, Fifth Forum, Oct., 1940*, pp. 130–33; *Ceram. Abs.*, **20** [4] 85 (1941).

[4] H. H. Holscher, "Measurement and Significance of Enamel Thickness," *Jour. Amer. Ceram. Soc.*, **19** [10] 298–303 (1936).

[5] R. L. Fellows, "Relation of Thickness to Impact Resistance of Porcelain Enamels," *ibid.*, **26** [5] 160–62 (1943).

[6] (*a*) C. J. Kinzie and J. A. Plunkett, "Use of Lindemann-Danielson Cross-Bending Test Machine," *ibid.*, **13** [9] 664–68 (1930).

(*b*) F. L. Meacham and E. F. Schweller, "Shell-Type Porcelain Enameled Refrigerator," *Better Enameling*, **7** [7] 8 (1936); reference from *Amer. Enameler* in Enamel Bibliography, 1944 ed., p. 186, has "Sweller" for "Schweller."

(*c*) "Data on Opacity and Cross-Bending Characteristics of Enamel," *Better Enameling*, **2** [11] 20 (1931).

(*d*) "Observations in Connection with Physical Tests for Enamels," *ibid.*, **2** [8] 28–30 (1931); Enamel Bibliography, 1944 ed., p. 204.

(*e*) "Old Timer Speaks on Chipping," *Enamelist*, **10** [7] 14 (1937).

[7] E. W. Dietterle, "Thin Coating, High Temperature Increase Enamel Strength," *Ceram. Ind.*, **36** [6] 62 (1941); *Ceram. Abs.*, **20** [11] 260 (1941).

[8] G. Gehlhoff and M. Thomas, "Brittleness of Opal Glass," *Jour. Soc. Glass Tech.*, **11**, 347–62 (1927); *Ceram. Abs.*, **7** [2] 72 (1928).

[9] J. B. Murgatroyd, "Testing of Commercial Glassware," *Jour. Soc. Glass Tech.*, **16**, 5–17 (1932); *Ceram. Abs.*, **11** [9] 487 (1932).

[10] R. L. Fellows and P. M. Wheeler, "Relation of Coefficient of Expansion to Impact Resistance of Porcelain Enamels," *Jour. Amer. Ceram. Soc.*, **24** [11] 356–60 (1941).

[11] M. C. Gautsch, "Relation of Coefficient of Expansion to Cross-Bending Strength of Sheet-Steel Enamels," *ibid.*, **15** [1] 8–12 (1932).

[12] (*a*) Richard Aldinger, "Causes and Prevention of Chipping of Enameled Cooking Utensils," tr. in *Ceram. Ind.*, **23** [3] 134–37 (1934); see Richard Aldinger, "Boiling . . .," Enamel Bibliography, 1944 ed., p. 3.

(*b*) Richard Aldinger, "Enamel Chipping on Rims and How to Prevent It," *Keram. Rundschau*, **43** [2] 25–28 (1935); *Ceram. Ind.*, **25** [1] 26–28 (1935); Enamel Bibliography, 1944 ed., p. 4.

[13] H. G. Wolfram and W. N. Harrison, "Effects of Composition on Properties of Sheet-Steel Enamels," *Jour. Amer. Ceram. Soc.*, **8** [11] 735–55 (1925).

[14] C. J. Kinzie and C. H. Commons, Jr., "Discussion of Thermal-Expansion Methods from Theoretical and Practical Standpoints," *ibid.*, **18** [10] 306–308 (1935).

[15] C. H. Wolff, "Construction of Refrigerator Linings," *ibid.*, **14** [2] 148–53 (1931).

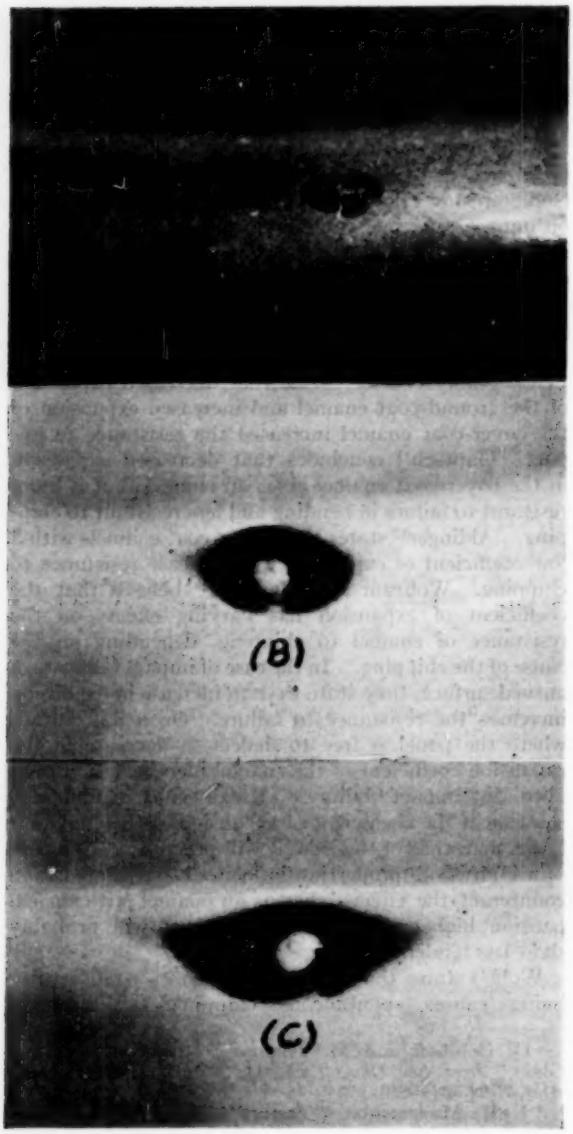

FIG. 1.—Effect of enamel thickness on size of chip formed on impact testing; enamel applied on 26-gauge pans. (A) One-coat gray mottled enamel (enamel thickness 0.0040 in., impact resistance 9.8 in.); (B) two-coat white enamel (enamel thickness 0.0090 in., impact resistance 13.6 in.); (C) three-coat white enamel (enamel thickness 0.0160 in., impact resistance 16.6 in.).

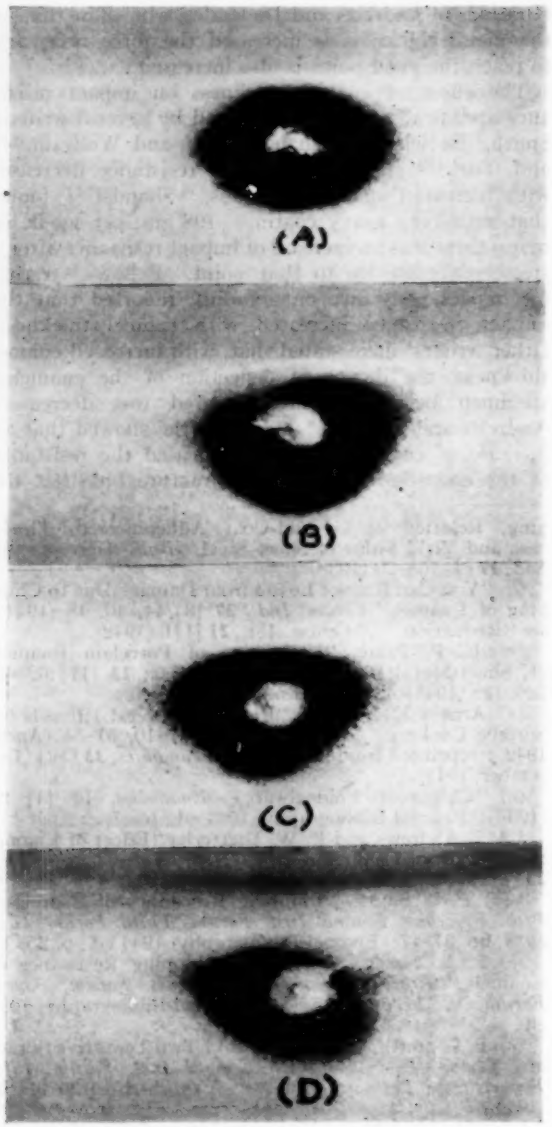

FIG. 2.—Effect of increase in metal thickness on size of chip formed on impact; all enamels, three-coat white; (A) metal thickness 0.0278 in., enamel thickness 0.0178 in., impact resistance 25.4 in.; (B) metal thickness 0.0220 in., enamel thickness 0.0198 in., impact resistance 24.8 in.; (C) metal thickness 0.0174 in., enamel thickness 0.0215 in., impact resistance 17.8 in.; (D) metal thickness 0.0115 in., enamel thickness 0.0220 in., impact resistance 13.0 in.

points out that an enamel of too low an expansivity, when applied to a bead, will result in spontaneous chipping.

Morey[16] states that glass may be broken by tension, compression, twisting, or impact but that the fracture always takes place in tension. Preston[17] sets forth the various types of fracture systems which are formed when glass is broken; he says,

> It is very important to remember that once a fracture starts the stress becomes radically redistributed and continues to redistribute itself as the fracture proceeds. The path varies with the magnitude and direction of the stress.

[16] G. W. Morey, Properties of Glass, p. 320. Reinhold Publishing Co., New York, 1938, 561 pp.; Enamel Bibliography, 1944 ed., p. 195.

[17] (*a*) F. W. Preston, "Study of Rupture of Glass," *Jour. Soc. Glass Tech.*, **10** [39] 234–69(1926); *Ceram. Abs.*, **6** [3] 97 (1927); see also **6** [9] 374 (1927).

(*b*) F. W. Preston, "Further Note on Fracture of System of Glass," *Jour. Soc. Glass Tech.*, **13** [49] 3–15 (1929).

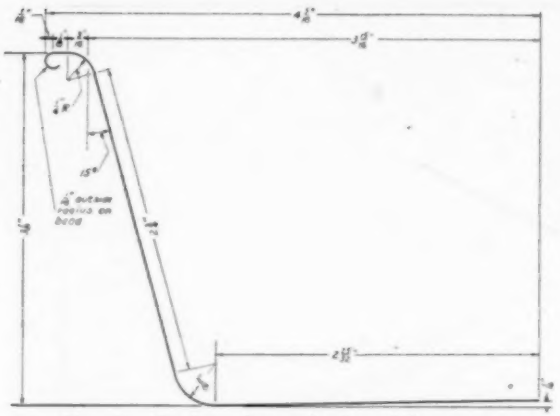

FIG. 3.—Design of standard pudding pan.

In another paper,[18] he states that the path of the fracture maintains itself at right angles to the direction of stress. In the same article, he also says,

> Glass is rarely broken in pure tension; more often it is broken by some sort of bending. One face of the glass, being in compression, tends to be free from many fractures, while the tension force has a family of fissures filling up the critical angle.

Preston[17(a)] recognizes the cone or hyperboloid fracture as the fracture which is formed on impact. This type of fracture is identified by the small hole on the side of the glass which was struck and a much enlarged hole on the other side of the pane. He states,

> The conical part may be extended considerably by increasing the pressure provided the glass is sufficiently thick.

[18] F. W. Preston, "Propagation of Fissures in Glass and Other Bodies with Special Reference to Split-Wave Front," *Jour. Amer. Ceram. Soc.*, **14** [6] 419–27 (1931).

The direction of the head of the flaw does not change much after the initial stage unless the flaw begins to approach another surface. Smith[3] reviewed the work of Preston and applied it to enamels. He classified chipping into two categories, (*a*) chipping that starts at the outer surface of the enamel and (*b*) chipping that starts within the enamel. Aldinger[12(a)] gives a good description of strain conditions within enamel layers.

III. Discussion of Chipping

As an introduction to this discussion, it will be advantageous to review the probable stress conditions of the enamel layers. The enamel layers, ground and cover coats, are in compression owing to the difference in the coefficients of expansion of the enamel and the steel. The extent of the stresses depends on this difference and on the thickness of the enamel layer.

Since this paper is concerned primarily with impact failures, this type of fracture will be discussed first. The typical impact failure is recognized by most enamelers by the cone of enamel which remains in the center of the impact area. This type of fracture is the cone or hyperboloid fracture, photographs of which are shown in Figs. 1 and 2. The force of the blow delivered by the impacting sphere is delivered at the area of contact of the sphere and enamel. This is a compressive force and does not ordinarily cause fracture, but the radial tension in the area about this point does cause a fracture when the force is great enough to rupture the enamel. The fracture changes its course from one perpendicular to the surface after the fracture starts because the stress conditions in the enamel layer change from what they were on the surface. The enamel

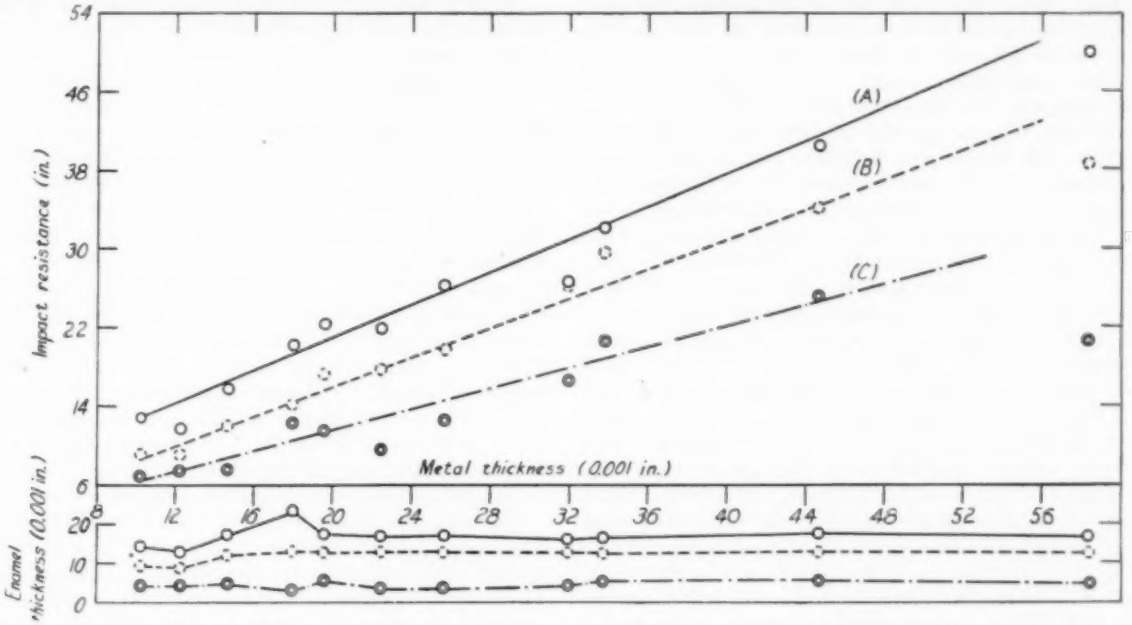

FIG. 4.—Effect of metal thickness on impact resistance (company X); test pans, two-quart pudding pans; (A) open circles, three-coat, avg. enamel thickness 0.0167 in.; (B) broken circles, two-coat, avg. enamel thickness 0.0119 in.; (C) open circles with center circle, one-coat gray, avg. enamel thickness 0.0045 in.

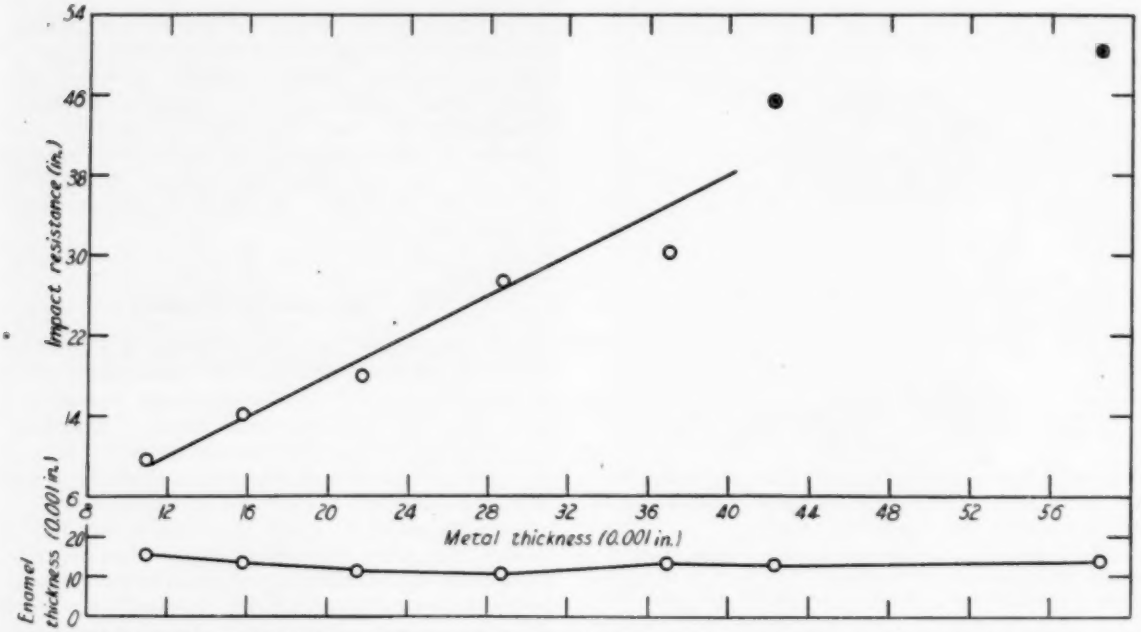

FIG. 5.—Effect of metal thickness on impact resistance (company Y); test pans, two-quart pudding pans coated with two coats of white over ground coat; avg. enamel thickness 0.0128 in.; circles with center dot indicate that ball was dropped from top of tube onto pan without causing failure on some of the spots that were impacted.

layers are in compression, and the metal layer is in tension owing to the difference between the coefficients of expansion. There is also a difference in the extent of compression in the ground- and cover-coat layers due to a difference in expansion, and it is reasonable to believe that a difference exists in stress condition through the enamel layers due to a possible interaction between the enamel layers at their interfaces during firing. This is especially true in the ground-coat layer where the enamel is in contact with the steel and the enamel composition is changed owing to solution of an iron oxide during firing. Since the stress conditions are changing, the path of the fracture changes so that it may remain perpendicular to the principal stress present. The center area broadens out as the fracture continues, and the fracture arrives at a point located generally in the ground-coat layer near the metal surface where the direction of the path is bent upward and starts toward the free surface of the enamel. As it approaches this free surface, the principal stress is perpendicular to that surface; the path tries to follow along this free surface and feathers out and eventually breaks through. The general shape of the piece chipped out is therefore circular or elongated, depending on the radius of curvature at the point of impact, with a hole in the center and thin on the outer circumference. Figure 1 shows that the size of the impact area is not constant; factors which influence this are the thickness of the enamel, the radius at the point of impact, and possibly the diameter of the pan. Figure 1 shows the great effect of the enamel thickness on the size of the chip where the thickness of the steel and the radius at the point of impact are constant. The chip is larger when the enamel coatings are thicker because the length of the possible path of travel of the fracture in a thicker layer is increased. Figure 2 shows four impact areas where the enamel thickness is approximately the same but the metal thickness varies; the size of the chip, however, shows little variation. This would indicate that the amount of stress necessary to cause the chip has no relation to the size of the chip since the stress necessary to cause fracture is increased as the metal thickness is increased.

When a blow is struck on a sharp radius, all of the energy of the blow is transferred to the enamel because such a point is very rigid and any deflection which occurs is slight. As the radius is increased, the possible deflection is increased and a portion of the energy of the blow is dissipated in the deflection of the steel and enamel. This deflection is an elastic deformation, and not a permanent distortion, and would cause the enamel to tend to fail at once. A flat panel would have greater deflection than a curved surface, and its resistance to impact therefore is much greater.

From the conditions present in impact, an enamel with a high coefficient of expansion would be expected to be more resistant to fracture by bumps or blows since the compression in such an enamel layer would be low. The effect of enamel thickness in this type of chipping is also important because, as the thickness of enamel increases the compressive stress in the enamel layer decreases, and the net effect is similar to that in an enamel of higher coefficient of expansion.

The physical characteristics of the cover coat are important in chipping due to impact. An increased bubble structure in a cover-coat enamel increases the resistance to impact failure since the thin enamel coating over the bubbles will be broken through and the enamel will be crushed, thus absorbing some of the force. With such a condition an increase in the ap-

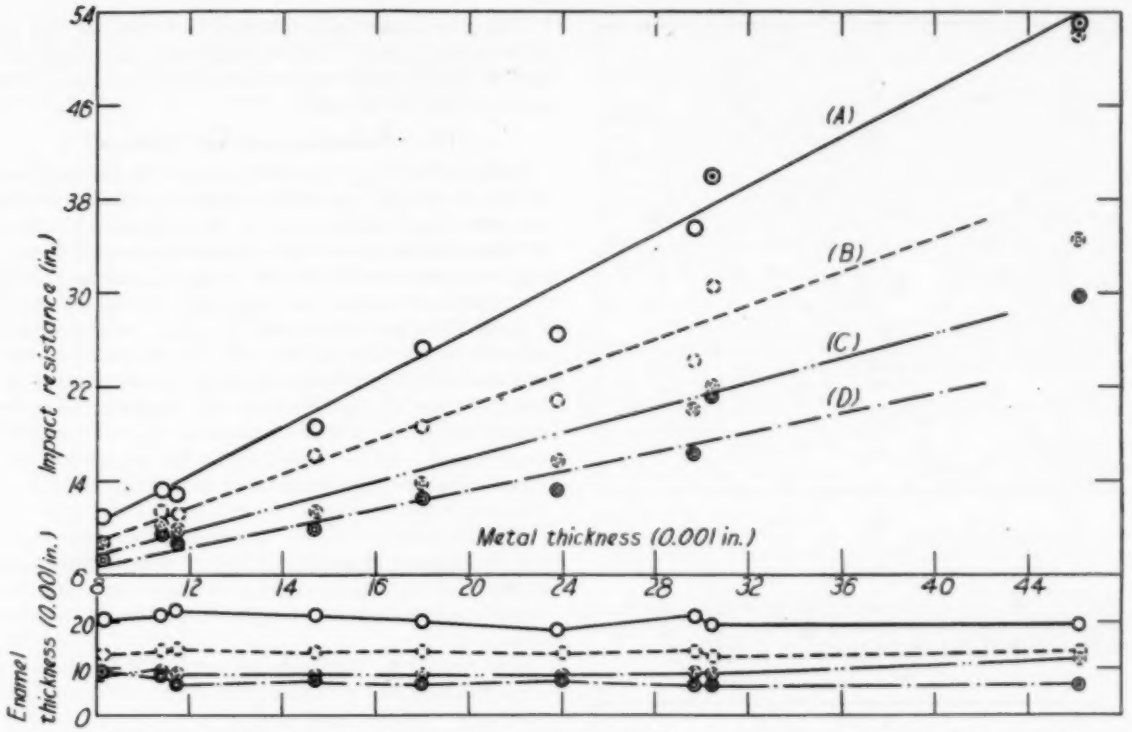

FIG. 6.—Effect of metal thickness on impact resistance (company Z); test pans, two-quart pudding pans; (A) open circles, three-coat, avg. enamel thickness 0.0205 in.; (B) broken circles, two-coat, avg. enamel thickness 0.0134 in.; (C) broken circles with center circle, one-coat speckled, avg. enamel thickness 0.0093 in.; (D) open circles with center circle, one-coat gray, avg. enamel thickness 0.0075 in.; open circles with dots, same as Fig. 5.

parent impact resistance of the enamel will be indicated. Because of other considerations, however, notably abrasion resistance, a bubbly structure should be avoided.

Chipping caused by bending or twisting is of an entirely different type and generally occurs on the outside of the bend. The resistance to deformation of enameling iron is known to increase as the thickness increases, and it also increases as the enamel coating increases in thickness, but in both cases the degree of deformation before fracture takes place is decreased. In bending a piece of enameled iron, there is a tensile stress on the convex surface of the piece, which causes the failure of the enamel; this failure shows up as cracks extending across the piece. These cracks occur in the critical angle of bending projected to the side which is in tension, and it is in this region that the enamel is chipped unless there is some flaw in the surface at some other point in which case the tensile stress will cause cracking there. Since the thicker enamel coatings cannot be deformed to as great an extent as thinner coatings without failure, the degree of deflection before fracture will be decreased. This is in agreement with published data obtained from cross-bend tests, but in most of these reports it is not pointed out that a greater stress is required to deform the test pieces to the failure point since no measurement of the amount of stress at failure was made.

It is advantageous to use an enamel with a low coefficient of expansion if it is to be subjected to bending because the enamel, in bending, does not fracture until the compression within the enamel layer has been overcome and changed to tension. After this point is reached, an increase of tensile stress causes fracture. The greater the compression within the enamel layer the greater must be the applied tensile stress before fracture occurs.

Thick enamel coatings are undesirable if a piece is to be subjected to bending since it cannot be deformed as much as a similar piece with a thin coating and, as the thickness of the coating is increased, the compressive stress within the layer is decreased. The structure of the cover-coat enamel is important since any possible flaws on the surface or in the enamel layer tend to weaken the coating in direct tension.

A third type of chipping occurs spontaneously and is most commonly seen on beads of enameled pans, on sharp radii, or at other points where there is a concentration of strain which may be caused by faulty design or construction. The tendency of this compressive strain is to relieve itself by popping off a piece of enamel, known as "spontaneous chipping." It is advantageous in such cases to use an enamel with a higher coefficient of expansion so as to reduce the compression in the enamel layer. Thick application of enamel is a contributing factor in spontaneous chipping. It is true that the thicker coat of enamel reduces the compression in the layer, but this type of chipping originates within the ground-coat layer or at the interface of the steel and ground coat and an in-

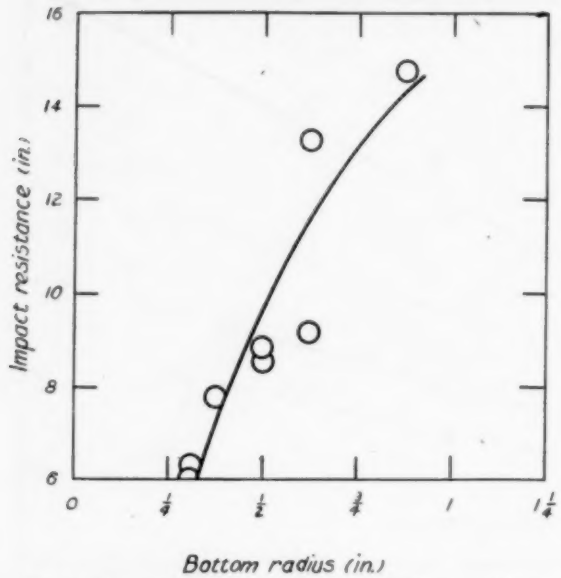

FIG. 7.—Impact resistance vs. bottom radius; specimens coated with one-coat mottled gray enamel; avg. enamel thickness 0.0061 in.; metal thickness 28-gauge.

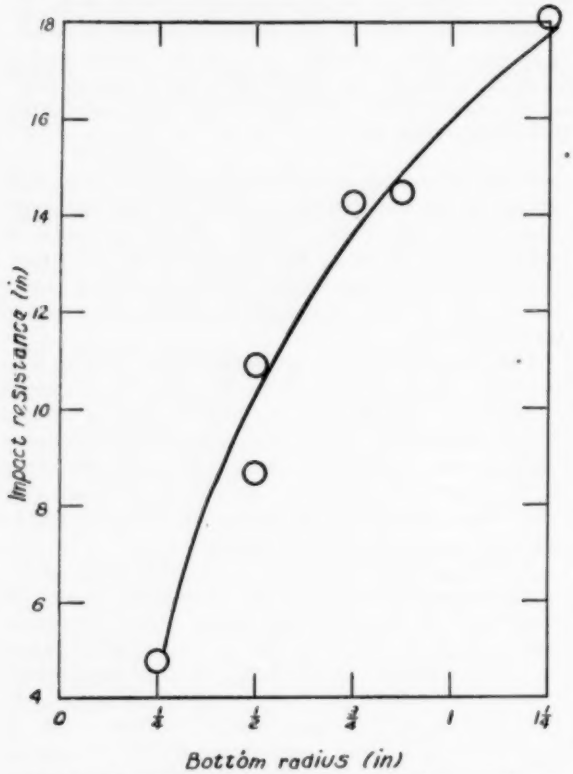

FIG. 8.—Impact resistance vs. bottom radius; specimens coated with one-coat blue speckled enamel; avg. enamel thickness 0.0053 in.; metal thickness 24-gauge.

crease in thickness of the coating increases the tensile stress normal to the radius, which is the stress that causes the failure.

This discussion has explained how various factors, such as metal and enamel thickness, enamel properties, and the design of the ware to be enameled, contribute to various types of chipping.

IV. Procedure and Test Methods

Standard two-quart pudding pans, of the design shown in Fig. 3, of different metal thickness and coated with one, two, and three coats of enamel were prepared by three manufacturers of commercial enameled cooking ware and were tested for impact resistance, using the standard impact test method[19] of the Enameled Utensil Manufacturers' Council. The test equipment was varied slightly in that the top of the tube was extended to obtain a drop of 51 in. rather than 35 in. For a study of the effect of the bottom radius on impact resistance, a series of pans having different radii were tested. Fifty impact spots, ten on each of five pans, were averaged to obtain the average impact resistance of the sample.

The thickness of enamel coating was measured with a G. E. magnetic thickness gauge.[20] The thickness was determined at four or more points on the inside and outside of the bottom of a pan and the values were averaged.

The metal thickness was determined on sections cut from the bottoms of eight pans for each different metal thickness. These enameled sections were then de-enameled in molten caustic, and the metal thickness was determined by measuring with a micrometer caliper. The average thickness of the eight pieces was then recorded as the metal thickness.

V. Test Results

The results of impact tests made on pans coated with one, two, and three coats of enamel submitted by company X are shown in Fig. 4. Eleven sets of pans of different metal thickness, ranging from 0.0103 to 0.0584 in., were tested. The two-, and three-coat pans were white, and the one-coat ware was a gray mottled enamel. Company Y submitted pans with three coats of enamel. The test results on these pans are shown in Fig. 5. Pans made with seven different thicknesses of steel were tested in this group. Company Z submitted pans coated with one-coat gray mottled, one-coat speckled black, two-coat white, and three-coat white; the test results are shown in Fig. 6. Nine different thicknesses of steel were tested in this group.

Figures 4, 5, and 6 show that in all cases the impact resistance increased with increase in metal thickness. The enamel thickness of each group of enamels is plotted on the lower curves. Curves *A*, *B*, and *C* in Fig. 4 represent three-, two-, and one-coat enamels, respectively. In Fig. 6, the same is true, and curve *D* is an additional one-coat enamel. The positions of these curves in relation to the horizontal axis show that an increase in enamel thickness increases the impact resistance.

[19] G. H. Zink and A. I. Andrews, "Enameled Utensil Manufacturers' Council Tentative Standard Impact Test for Porcelain Enameled Cooking Utensils," *Bull. Amer. Ceram. Soc.*, **22** [8] 283–86 (1943).

[20] "New G. E. Thickness Gage for Curved or Plane Surfaces," *Better Enameling*, **10** [1] 28 (1939).

Figures 7 and 8 show the results of impact tests made on two groups of pans having different bottom radii. The impact resistance increased with increase of the bottom radii in both series of pans.

VI. Discussion of Results

Figures 4, 5, and 6 show that the impact resistance increased with increases in enamel thickness and also with an increase in the metal thickness. These curves were plotted as straight lines because there were insufficient data on pans with a metal thickness of over 0.035 in. from which to predict the exact shape of the curve in that region. It is believed, however, that with increased metal thickness the curves would turn up sharply. The points marked with plus signs indicate that some of the individual tests that were averaged with the other values exceeded a drop of 51 in., which was the length of the tube.

Figures 7 and 8 show that an increase in the bottom radius of a pan increases the impact resistance.

Figure 1 shows that the size of the chip formed on impact increases with an increase of enamel thickness. This is an important consideration since it lessens the desirability of attempting to increase impact resistance by increasing enamel thickness.

VII. Summary of Results

Impact tests made, using the standard method of the Enameled Utensil Manufacturers' Council, indicate that (1) increases in enamel thickness increase resistance to impact; (2) increases in the size of the bottom radius give increased resistance to impact; (3) increases in the thickness of the metal stock increase the impact resistance; and (4) the size of the chips formed by impact on enamel radii is greater as the thickness of the enamel layer is increased.

Bibliography References

1. F. W. Preston, "Shooting Through Glass with a Rifle," *Jour. Soc. Glass Tech.*, **11**, 283–86 (1927); *Ceram. Abs.*, **7** [2] 71 (1928).

2. Otto Graf, "Impact Tests on Glass," *Glastech. Ber.*, **6** [10] 582–84 (1928); *Ceram. Abs.*, **8** [9] 641 (1929); *Ceram. Abs.* gives year of *Glastech. Ber.* reference as 1929, which is incorrect.

3. J. T. Littleton and F. W. Preston, "Theory of Strength of Thermally Toughened Glass," *Jour. Soc. Glass Tech.*, **13**, 336–49 (1929); *Ceram. Abs.*, **9** [7] 513 (1930).

4. F. W. Preston, "Impact Modulus of Glass," *Jour. Amer. Ceram. Soc.*, **14** [6] 428–31 (1931).

5. F. W. Preston, "Brief Analysis of Some Recent Data on Impact Strength of Glass," *ibid.*, **14** [6] 432–34 (1931).

6. F. W. Preston, "Stresses in Wire Glass Due to the Wire," *ibid.*, **14** [6] 435–40 (1931).

7. F. W. Preston, "Form of Cracks in Bottles," *ibid.*, **15** [3] 171–75 (1932).

8. F. W. Preston, "Note on Concept of Brittleness," *ibid.*, **15** [3] 176–78 (1932).

9. F. W. Preston, "Glass as Structural and Stress-Resisting Material," *ibid.*, **16** [4] 163–86 (1933).

10. F. W. Preston, "Angle of Forking of Glass Cracks as Indicator of Stress System," *ibid.*, **18** [6] 175–76 (1935).

11. F. W. Preston, "Time Factor in Testing Glass," *ibid.*, **18** [7] 220–24 (1935).

12. O. Bartsch, "True and Apparent Impact Strength (of Ceramic Materials)," *Ber. Deut. Keram. Ges.*, **17**, 281–85 (1936); *Ceram. Abs.*, **16** [4] 125–26 (1937).

13. B. Moore, "Impact Strength of Transparent and Translucent Fused Silica and Recrystallized Alumina," *Jour. Soc. Chem. Ind.*, **59**, 119–20 (1940); abstracted in *Jour. Soc. Glass Tech.*, **23**, 234 (1940).

14. "Impact Tests on Glass Tile," *Engineering*, **150** [3889] 66 (1940); *Ceram. Abs.*, **20** [1] 12 (1941).

Acknowledgment

This investigation was carried out in the Department of Ceramic Engineering at the University of Illinois and was financed by the Enameled Utensil Manufacturers' Council of Cleveland, Ohio. The authors wish to express their appreciation to the members of the Technical Committee of the Council, consisting of E. C. Dexheimer, H. C. Arnold, E. H. Kelsey, B. S. Kirk, P. A. Mallonn, and A. J. Vollrath for their advice, suggestions, and cooperation.

Department of Ceramic Engineering
University of Illinois
Urbana, Illinois

FUNDAMENTAL PROPERTIES OF RAW CLAYS INFLUENCING THEIR USE*

By C. G. Harman and C. W. Parmelee

Abstract

Several properties of single-base clays were measured to test the general correlation of these properties. This correlation is possible providing the water content and the soluble constituents are controlled, in which case the properties can be defined as functions of sorption capacity, the nature of the adsorbed ions, and the pore structure.

I. Introduction

(1) Objective and Review

The object of this investigation was to obtain information to form the foundation for the general correlation of the properties of clays. It was believed that more could be learned by a general study of many properties than from a detailed study of a few. The ultimate objective, not achieved within the scope of the immediate problem, was to obtain information that would facilitate the selection of clays for specific purposes and to enable better control in use.

Endell, Hofmann, and Wilm[1] made an extensive investigation of the relation between some properties of natural clays (not single-base clays) and base-exchange capacity. Several properties of natural kaolins have been correlated with base-exchange capacity by Klinefelter and his co-workers.[2] Endell and Vageler[3] investigated the relationship between adsorbed cations and the water content of ceramic clays.

These workers were able to demonstrate at least a qualitative relationship between the ceramic properties investigated and the base-exchange capacities of the different clays. The relation was evident in spite of uncontrolled variables, such as particle size, mineralogical composition, chemical composition, and cation species. Such data support the theory that surface phenomena are of primary importance in clay–water systems.

Many studies relating to ionic exchange (Mattson,[4] Ramann and Spengel,[5] Bradfield,[6] and Ganssen[7]) have characterized the process by dissociation constants and true chemical reactions. Jenny[8] and Cooper[9] have studied sorption phenomena from the standpoint of participating ions. This viewpoint seems particularly practical because the ions remain ionized even after adsorption and the properties of surfaces will be largely dependent on properties of the adsorbed ions.

(2) Mechanism of Adsorption

Adsorption results from mutual attraction between ions or ionized groups in the surfaces of the solid phases and the ions or charged groups in the surrounding phase. The adsorptive power of clays thus originates from the ultimate structure of solid matter present, the active portions of which are in the exposed surfaces. According to Jenny,[8(b)]

> The places of attraction in colloidal particles are the negative O^{--} and OH^{-} ions in the rigid crystal frame. Only positive ions will adhere; negative ions, as a rule, will be repelled and remain in the surrounding liquid. The intensity of fixation follows Coulomb's law according to which the attraction is directly proportional to the product of the charges of the ions and indirectly proportional to the square of the distance between charges, which of course is determined by the size of the ions. Wiegner's[10] contribution in base-exchange studies consists in the introduction of the size of the hydrated ions instead of "crystal ions" in Coulomb's equation. . . . The K ion with its thin water shell can go closer to the O ion of the crystal frame than the more highly hydrated Na ion. The attraction between the negative inner layer and the K ion is therefore greater than for the sodium ion; in other words, K is better adsorbed than Na, and held more tightly.

---

* Presented at the Forty-First Annual Meeting, The American Ceramic Society, Chicago, Ill., April 18, 1939 (Materials and Equipment Division). Received August 26, 1944.

Based on a thesis submitted by the senior author in partial fulfillment of the requirements for the degree of Doctor of Philosophy in Engineering in the Graduate School, University of Illinois, Urbana, Ill., June, 1939.

[1] K. Endell, U. Hofmann, and D. Wilm, "Über die Natur der keramischen Tone," *Ber. Deut. Keram. Ges.*, **14** [10] 407–38 (1933); *Ceram. Abs.*, **13** [4] 101 (1933).

[2] T. A. Klinefelter, W. W. Meyer, and E. J. Vachuska, "Some Properties of English China Clays," *Jour. Amer. Ceram. Soc.*, **16** [6] 269–76 (1933).

[3] Kurd Endell and P. Vageler, "Kationen- und Wasserhaushalt keramischer Tone in rohen Zustand," *Ber. Deut. Keram. Ges.*, **13** [9] 377–411 (1932); *Ceram. Abs.*, **12** [5] 206 (1933).

[4] Sante Mattson, "Beziehungen zwischen Ausflockung, Adsorption, und Teilchenladung mit bes. Berücksichtigung der Hydroxylionen," *Kolloidchem. Beihefte*, **14**, 227–313 (1922); also series of articles in *Soil Science* by same writer.

[5] E. Ramann and A. Spengel, "Über den Basenaustausch der Silikate," *Z. Anorg. Allgem. Chem.*, **95**, 115–28 (1916); **105**, 81–96 (1919); **114**, 90–104 (1920).

[6] Richard Bradfield, "Some Chemical Reactions of Colloidal Clay," *Jour. Phys. Chem.*, **35** [1] 360–73 (1931); *Ceram. Abs.*, **10** [4] 300 (1931).

[7] R. Ganssen, "Über die chemische oder physikalische Natur der kolloidelen wasserhaltigen Tonerdesilikate," *Centr. Mineral.*, A, pp. 699–712, 728–41 (1913).

[8] (*a*) G. Wiegner and H. Jenny, "On Base Exchange," abstracts of *Proc. 1st Internat. Congr. Soil Sci. Commission*, **II**, pp. 46–51 (1927).

(*b*) H. Jenny, "Behavior of Potassium and Sodium During Process of Soil Formation," *Univ. of Mo. Agric. Expt. Station Research Bull.*, No. 162, 63 pp. (1931).

[9] H. P. Cooper, "Ash Constituents of Pasture Grasses, Their Standard Electrode Potentials and Ecological Significance," *Plant Physiology*, **2**, 193–214 (1930).

[10] G. Wiegner, "Dispersital und Basenaustausch (Ionenaustausch) Zsigmondy Festschrift," *Kolloid-Beihefte*, **36**, 341–69 (1925).

TABLE I

PRESSURES EXISTING IN WATER AT VARIOUS DISTANCES FROM ION (ACCORDING TO WEBB[14])

Distance from ion (a.u.)*					
12.77	5.76	4.16	3.09	2.32	1.95
Field strength†					
10^4	5×10^4	10^5	2×10^5	4×10^5	6×10^5
Pressure‡					
0.43	20.9	1.76×10^3	1.28×10^3	6.34×10^3	1.24×10^4

* Distance (a.u. from center of ion).
† Values of internal field strengths corresponding in c.g.s. electrostatic units.
‡ Pressure (megadynes/sq. cm.).

TABLE II

CONTRACTION OF SOLVENT PRODUCED BY IONS OF VARIOUS RADII (ACCORDING TO WEBB[14])

Radius (a.u.)									
4.165	3.090	2.318	1.948	1.715	1.551	1.285	1.122	0.924	0.804
Contraction (cc.)*									
1.40	3.59	7.66	10.27	11.84	12.86	14.21	14.83	15.44	15.69

* Contraction, total decrease in volume (cc.) attending solution of 1 mole of ions in infinite quantity of water, as calculated for ions of various radii.

Every ion is surrounded by a shell of oriented water; the ions are hydrated. The mechanism of the hydration phenomenon has been described by Born,[11] Drude and Nernst,[12] Washburn,[13] and Webb.[14] The free energies of hydration of chemically unhydrated ions have been obtained as a function of ion radii by calculating the difference in energy necessary to charge the ion in a vacuum and that necessary to charge the ion in water and to compress the solvent in the vicinity of the ion. The field strength of an ion is crudely proportional to the charge of the ion divided by the square of its radius.

Water, being a permanent dipole, is tremendously influenced by the presence of ions. Under the influence of an electric field, water molecules become oriented and more tightly packed, forming a "shell" around the ion. Properties of ions of importance in this connection are shown in Tables I, II, and III. The amount of water attracted by an ion is directly proportional to the field strength of the ion and the amount of free water available. Thus, Na^+ will attract more water than K^+; and H^+, more water than Na^+. The amount of water associated with ions has been studied by Washburn[13] who reports 18.0 mols of H_2O per ion of Na and 11.5 mols of H_2O per ion of K.

TABLE III

FREE ENERGIES OF HYDRATION OF INDIVIDUAL IONS (ACCORDING TO WEBB[14])

Ion						
Na^+	K^+	H^+	Zn^{++}	Ca^{++}	Mg^{++}	Al^{+++}
Radius (a.u.)						
1.505	1.873	0.8	1.04	1.06*	0.78*	0.57*
Free energy of hydration (kg.-cal./gm.-ion)						
99	81.7	249.6	525	349.0†	459†	

* According to Goldschmidt, for crystals.
† Cited by P. Vageler and F. Alten, "Soils of the Nile and Gash," *Z. Pflanzenernähr. Düngung Bodenk.*, **21A**, 323–46 (1931); p. 335.

(3) Application of Fundamentals to Ceramic Clays

It is convenient to cast the properties of clays into three main groups, as follows, based on the fundamental factors involved:

Group I: Compositions, (*a*) Mineralogical composition: types and relative amounts of mineral species, (*b*) physical compositions: particle sizes, distributions, and shapes of each mineral; and (*c*) chemical composition.

Group II: Properties or factors derived from group I: (*a*) adsorption phenomena and (*b*) the packing and textural characteristics.

Group III: Those physical properties controlled by (*a*) or (*a*) and (*b*) of group II: (*a*) dry strength, (*b*) drying shrinkage, (*c*) plasticity, (*d*) flow characteristics of suspensions, (*e*) stability of suspensions, (*f*) drying behavior, (*g*) permeability, and others.

The behavior of raw clays accordingly should be defined by an adequate measurement of the pore space of the dried clays and by their ion-sorption capacity, if the soluble constituents are controlled. If these conditions can be shown to apply, a simplified procedure for examining clays and bodies and correlating their properties could be developed.

II. Experimental

(1) Samples and Preparation

Samples were selected for the study of as wide a range of types as possible within the scope of the in-

[11] (*a*) M. Born, "Volumn und Hydrationswärme der Ionen," *Z. Physik*, **1**, 45–48 (1920).
(*b*) M. Born, "Über die Beweglichkeit der Electrolytischen Ionen," *ibid.*, **1**, 221–49 (1920).
[12] P. Drude and W. Nernst, "Über Elektrostriktion durch Freie Ionen," *Z. Physik. Chem.*, **15**, 79–85 (1894).
[13] E. W. Washburn, "Neueren Forschungen über die Hydrate in Lösung," *Jahrb. Radiokt. Elektronik*," **5**, 493–552 (1908); **6**, 69–123 (1909).
[14] T. J. Webb, "Free Energy of Hydration of Ions and Electrostriction of Solvent," *Jour. Amer. Chem. Soc.*, **48**, 2589–2603 (1926).

TABLE IV

LIST OF SAMPLES STUDIED, MINERAL COMPOSITIONS, AND SOURCE

Sample	Source	Mineralogical composition
N. C. kaolin	N. C.	Chiefly coarse kaolinite; some muscovite, quartz, and orthoclase
English china clay	England	Chiefly coarse kaolinite; white mica, quartz, and feldspar
Ga. kaolin	Ga.	Chiefly kaolinite
Fla. kaolin	Fla.	Kaolinite, traces of quartz
Tenn. ball No. 7	Tenn.	Kaolinite, some illite
Tenn. ball No. 5	Tenn.	Kaolinite, some illite; quartz, organic material, lignite
Vallendar clay	Germany	Kaolinite and illite; quartz, muscovite, and feldspar
Alton clay (No. 2 fire clay)	Alton, Ill.	Kaolinite, some illite and organic matter, quartz and pyrite
Texas clay	N. Mex.	Kaolinite and montmorillonite; some unidentified mineral probably allophane
Peat	Northern Ill.	Chiefly lignite; some quartz, kaolinite, and other minerals
Bentonite	Wyo.	Montmorillonite

vestigation. A list of the samples and a description of their mineral compositions are given in Table IV.

Quantities of each sample were converted to hydrogen clay by leaching or by electrodialysis with an apparatus similar to one described by Bradfield.[15] These samples were air dried and sealed in jars until needed. Portions of some of the clays were treated with H_2O_2 to remove the organic matter.

Sodium clays were prepared by adding NaOH to the hydrogen clays in amounts equivalent to the respective base-exchange capacities.

(2) Methods of Measuring Properties

(*A*) *Base-Exchange Capacity:* The base-exchange capacities were determined by the ammonia distillation method. The clays were leached with normal neutral ammonium acetate solution, and the excess ammonium acetate was removed by washing with neutral absolute methyl alcohol. The adsorbed NH_4^+ was replaced by washing with 0.1 *N* HCl and the displaced ammonia determined by the Kjeldahl method.

(*B*) *Heat of Wetting:* Heat of wetting was determined by a method described by Janert.[16] The apparatus consisted of a Dewar flask, suspended inside another larger (Dewar) flask. It was covered by a well-insulated lid, bored to accommodate a Beckmann thermometer, a stirrer, and the sample bottle.

The calorimeter was charged with a quantity of water such that the volume of the water plus the volume of the sample was always 300 cc. Samples were dried

[15] Richard Bradfield, "Inexpensive Cell for Purification of Colloids by Electrodialysis," *Ind. Eng. Chem.*, **20**, 79–80 (1928).

[16] H. Janert, "Application of Heat-of-Wetting Measurements to Soil Research Problems," *Z. Pflanzenernähr. Düngung u. Bodenk.*, **19A**, 281–93 (1931); **34A**, 100–108 (1934).

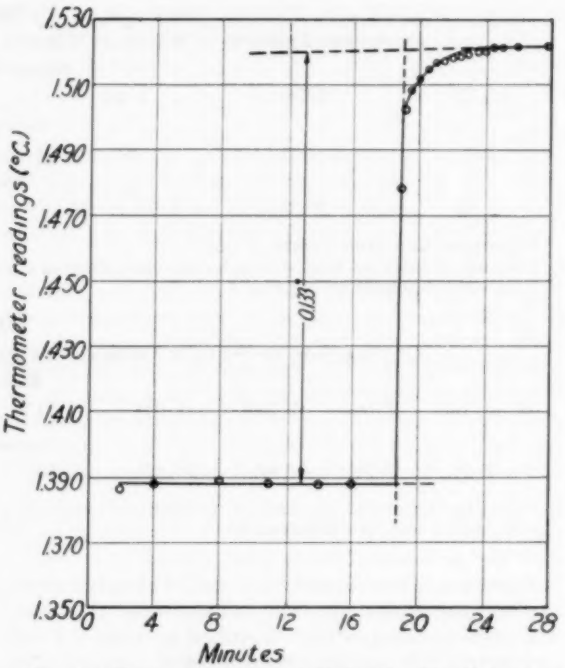

FIG. 1.—Heat of wetting of H kaolin (English china clay); weight of sample dried at 105°C., 39.847 gm.; heat of wetting, 1.04 cal. per gm.

at 105°C., weighed in glass capsules provided with ground-glass caps, which were then sealed with paraffin. The sealed sample was immersed in the water in the calorimeter and allowed to stand overnight to attain thermal equilibrium. When ready to make the test, the water in the calorimeter was gently stirred, and a record was kept of the temperature and time. The sample bottle was quickly removed, the clay was dumped into the calorimeter, and the temperatures were read so that curves such as Fig. 1 could be plotted. Heats of wetting were calculated from the temperature rise, weight of sample, and apparatus constant. The calorimeter was calibrated by the heat of solution of sodium carbonate.

(*C*) *Measurement of Hydrogen-Ion Concentration:* The clays were mixed with water to form a thick slip containing 0.5 gm. of clay per cc. of slip. A Beckmann pH meter was used in the determinations.

(*D*) *Equilibrium Moisture:* For the purpose at hand, the ordinary desiccator method was used in which the clay samples were brought to equilibrium with the vapor above sulfuric acid solutions of appropriate concentrations. This method is open to criticism in several respects, but it proved to be satisfactory for the purposes of this investigation. The samples were left in contact with the vapor for six months at approximately 25°C.

(*E*) *Permeability:* In order to obtain a comparison of the relative permeabilities of the various clays, the following tests were devised.

(i) *Method No. 1:* A 10-gm. sample of clay was weighed to an accuracy of ±0.05 gm.; 50 cc. of distilled water were added to the sample, and the suspension

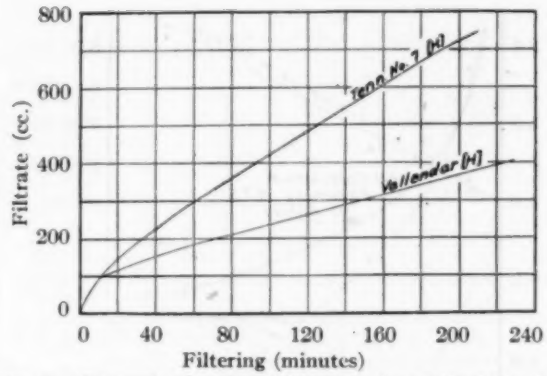

FIG. 2.—Example of permeability data by method No. 2.

was allowed to stand 12 hours. A 9-cm. Büchner funnel was prepared, using No. OK filter paper, and was made to set as nearly level as possible. A vacuum of 29 in. was applied and the suspension transferred to the funnel. Ample time was allowed for the clay layer to form; the vacuum was then released, and a graduated cylinder was placed inside the flask so that the funnel when replaced had its spout inside this cylinder. The vacuum was again applied, and records were made of the time required for 5.0 cc. of liquid to pass through the clay membrane. The temperature during all runs was near 24°C.

(ii) *Method No. 2:* Ten grams of clay were added to 50 cc. of distilled water in a flask, agitated 72 hours with a mechanical agitator, and transferred to a Büchner funnel. The time required for 20-cc. portions of distilled water to pass the clay membrane was noted. Figure 2 shows an example of the type of data obtained by this method.

(iii) *Method No. 3:* Ten grams of clay and 50 cc. of water were put into a flask and deflocculated by additions of NaOH. After 72 hours of mechanical agitation, the sample was flocculated by a few drops of HCl and transferred to the funnel, the chlorine ions were leached, and the filtration rate was measured.

(*F*) *Rate of Drying:* The clays were made plastic, adjusted to a plasticity number of about 1.5,[17] and then formed into cylindrical test specimens. These specimens were 1 sq. in. in cross section with height equal to the diameter. These were set on the laboratory table and weighed periodically to determine the rate of water loss. This simple test was all that could be carried out with the limited amount of sample available and with clays of so wide a range of drying characteristics.

(*G*) *Drying Shrinkage:* Drying shrinkage was measured on the "rate-of-drying" samples. The plastic volumes were determined by weighing suspended in carbon tetrachloride. Dry volumes were calculated from the weights of bars saturated and suspended in carbon tetrachloride.

(*H*) *Porosity Measurements:* The porosity of dried bars was calculated from their respective dry volumes, weights, and true densities.

(*I*) *Dry Strength:* The compressive strengths were determined with a small hydraulic press on specimens approximately 1 in. in diameter and 1 in. high. For modulus of rupture, specimens $^1/_2$ in. in diameter were loaded at the midpoint of a span of 6 cm.

III. Results and Conclusions

(1) Base-Exchange Capacity

The base-exchange capacities are shown in Table V. These data will be used as a function against which the other properties are plotted to test correlation inasmuch as all properties which are functions of base-exchange capacity are also functions of, or are related to, each other.

TABLE V
BASE-EXCHANGE CAPACITIES

Sample	Base-exchange capacity (m.e./100 gm.)
N. C. kaolin	4.0
S. C. kaolin	4.9
English china clay	5.9
Fla. kaolin	8.0
Tenn. ball clay No. 7	10.2
Tenn. ball clay No. 5	12.1
Vallendar clay	13.8
Alton clay	21.9
Alton clay (treated with H_2O_2)	20.3
Texas clay	33.3
Peat	76.7
Bentonite	85.1

The identity of the individual clays will not be indicated on most of the graphs, but they may be recognized by their base-exchange capacity values by reference to Table V.

(2) Heat of Wetting

Heat-of-wetting data can be very useful in clarifying the mechanism of adsorption by clays. Janert,[16] reasoning that polar adsorption should be closely correlated with exchangeable bases and consequently the heat of hydration* of adsorbed cations, was able to show that the ratio of heat of hydration of the adsorbed ions to the heat of wetting is a constant. His values for these ratios are as follows: H clays 11.5, Mg clays 9.0, Ca clays 7.0, K clays 5.1, and Na clays 4.9. These ratios will vary some with concentration as shown in section III (3) on pH.

The results were taken as proof that the adsorbed ions are the source of the activity in clay–water systems. Since the cations are more or less associated with solid-phase surfaces, only a certain fraction of the total heat of hydration can reappear when the dry clay is wetted. This proportion differs considerably for

[17] Cylindrical test specimens were subjected to simultaneous compression and torsion by means of an apparatus described by Endell (see Kurd Endell, H. Fendius, and U. Hofmann, "Basenaustauschfähigkeit von Tonen und Formgebungsprobleme in der Keramik," *Ber. Deut. Keram. Ges.*, **15** [12] 595–625 (1934); *Ceram. Abs.*, **14** [6] 149 (1935)). The plasticity number was the product of the deformation and the load at the time of rupture.

* Heat of hydration of the ion at infinite dilution. Some relationships between ionic radii and hydration are shown in section II (2), p. 112, and in Tables I, II, and III. The values used in this work for heats of hydration are given in Table III.

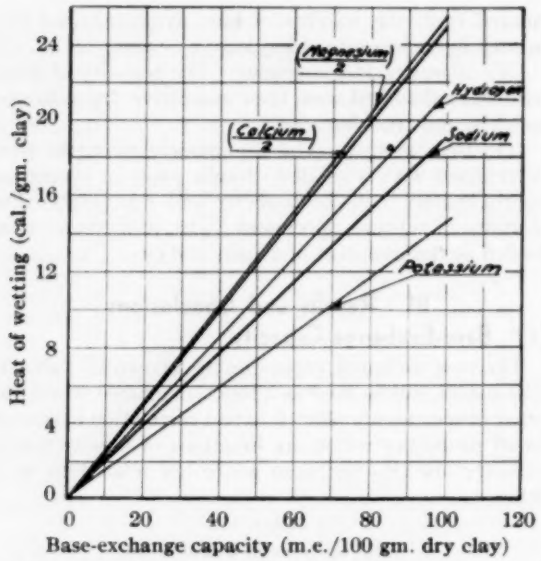

FIG. 3.—Relation between heat of wetting of clays and adsorbed cations; curves calculated from data by Janert[18]; points show data on H clays obtained in present investigation.

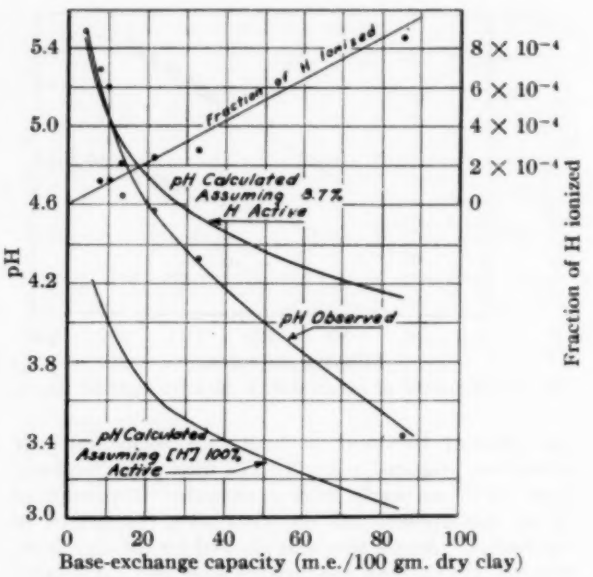

FIG. 4.—Hydrogen-ion concentration of H^+ clays.

the different cations. The adsorption is strongest for hydrogen, and therefore only 1/11.5 (8.7%) of the total heat is returned as heat of wetting. Sodium is but little adsorbed and 1/4.9 (20%) appears in the heat of wetting. Other cations fall between and follow the well-known order of intensity of adsorption.

The values of heat of wetting used in constructing the curves plotted in Fig. 3 were calculated by equation (1).

$$\text{Base-exchange capacity} = \frac{100\,K \times \text{heat of wetting}}{\text{Heat of hydration}} \qquad (1)$$

K = Janert's ratio of heat of hydration to heat of wetting.

This ratio was checked in the present investigation for three H clays, the values being indicated in Fig. 3.

Perhaps the most important application of this generalization is the prediction of the behavior of cations in clay–water systems. The greater the portion of ionic energy used up in its adsorption by the colloid, the closer the system approaches an isoelectric point; conversely, cations retaining a high percentage of their energy should be good dispersing agents. It is possible to evaluate these factors precisely and conveniently by heat-of-wetting measurements.

(3) Hydrogen-Ion Data

The pH data were interpreted in the same manner as heat of wetting. If none of the energy of hydrogen ions were utilized in adsorption, the pH would be the same as computed for the 100% ionized chemical system (as shown in Fig. 4) by the curve labeled "pH calculated assuming 100% of H^+ active." The curve calculated assuming 8.7% (Janert's factor) of H^+ active is much closer to the observed values. These values could not be expected to check with those calculated from the 8.7% factor since the water-to-clay ratios are radically different in the two cases. The heat-of-wetting measurements were taken at practically infinite dilution (considering only the ions), whereas the pH measurements were made on samples containing 0.5 gm. of clay per cc. of suspension. The difference between the computed and observed pH values simply means that the intensity of adsorption of the cations varies with water content. The degree of change on addition of a given quantity of electrolyte per gram of clay would not be the same for plastic clay and a slip made of the same clay.

The method of calculation of pH is obvious from Table VI. The fraction of hydrogen ionized and the dissociation constants were calculated according to the usual means of the physical chemist. These calculations involve the assumption that clay acts as a polyvalent acid in which the silicate is the anion and the adsorbed hydrogen the cation.

If pH is to be used as a control in clay work, the relations apparently must be determined empirically for each individual case. The same pH, of course, can be obtained in solutions containing a variety of different cations. Since the behavior of clay–water systems is dependent on the particular type of cation present, pH in polyionic systems may be incidental and not fundamental unless adequate additional data are at hand.

(4) Equilibrium Moisture

The equilibrium moisture of several H clays is shown in Fig. 5. This is tantamount to plotting equilibrium moisture against the vapor pressure of the equilibrium moisture. The drop in vapor pressure as the moisture content decreases shows that the water is under strong restraining influence due to the attraction by the adsorbed cations. The relationship between the base-exchange capacities of clays and hygroscopic moisture is shown in Fig. 6.

The amounts of moisture (hygroscopic) adsorbed by the different samples and in equilibrium with atmos-

TABLE VI

HYDROGEN-ION CONCENTRATION OF H CLAYS, OBSERVED AND CALCULATED

	a*	b†	Log 1/b‡	pH observed	L§	K‖
N. C. kaolin	4 × 10^{-5}	34.8 × 10^{-7}	5.46	5.5		
Fla. kaolin	8 " "	69.0 " "	5.15	5.30	1.25 × 10^{-4}	0.625 × 10^{-9}
Tenn. No. 7 ball	10.2 " "	88.7 " "	5.05	5.21	1.26 " "	0.80 " "
Vallendar clay	13.8 " "	119.7 " "	4.92	4.65	2.18 " "	3.26 " "
Alton clay	21.8 " "	189.7 " "	4.72	4.58	2.42 " "	5.85 " "
Texas clay	33.3 " "	290 " "	4.54	4.33	2.80 " "	13.1 " "
Bentonite	85.3 " "	742 " "	4.13	4.43	8.73 " "	340.8

* *a*, equiv. of H/gm. of clay.
† *b*, equiv. of H/gm. of clay × 0.087 (0.087, Janert's factor for heat of wetting).
‡ Log 1/*b*, calculated pH.
§ *L*, fraction of H ionized (calculated).
‖ *K*, dissociation constant (calculated).

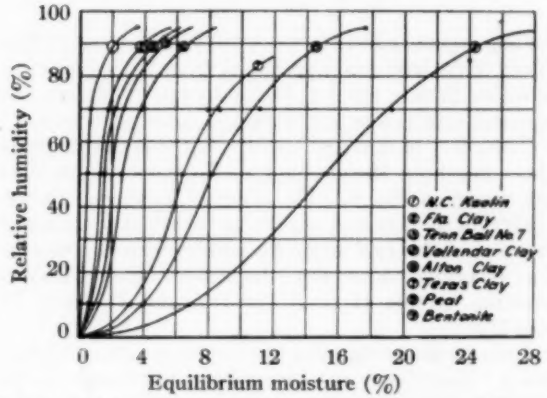

FIG. 5.—Moisture in equilibrium with H clays at different relative humidities.

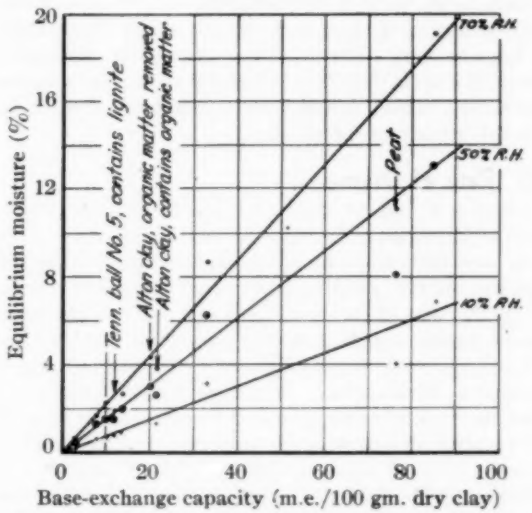

FIG. 6.—Moisture in equilibrium with various H clays at different relative humidities at 25°C.; R.H. indicates relative humidity.

pheres of 10, 50, and 70% relative humidity at 25°C. is plotted against the base-exchange capacities of the respective clays in Fig. 6. These curves were constructed from the same data used for plotting Fig. 5, and from data on two additional clays. With certain exceptions, there is excellent linear correlation. The Texas clay (base-exchange capacity 33.3, Table V) does

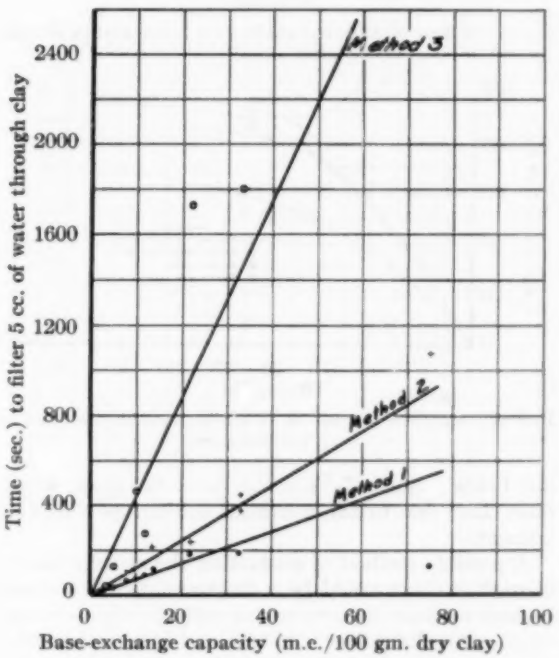

FIG. 7.—Permeability of H clays at 25°C.

not correlate on any of the curves. All other points not correlating are low, and all these samples contain an appreciable amount of organic matter. The sample of peat has a very low hygroscopic water content per exchangeable ion. Clays high in organic matter seem to be characterized by lower moisture-adsorption capacity as is illustrated by the fact that the Alton clay (base-exchange capacity 21.9) falls below the curve, but the same clay after removal of the organic matter (base-exchange capacity 20.3) falls on the curve. A similar reaction was observed in the case of Tenn. No. 5 ball clay.

Organic material in clay is somewhat soluble, and some of it apparently dissociates to form ions of a character quite different from hydrogen. The well-known characteristic of lignitic clays to disperse in water has never been explained. The postulation that organic matter dissolves and ionizes to produce some ionized groups of low field strength would explain the anomalies found here as well as others to be pointed

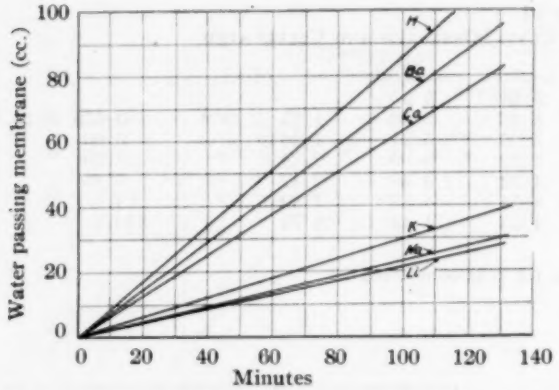

FIG. 8.—Effect of different cations on permeability of clay (after Lutz[18]).

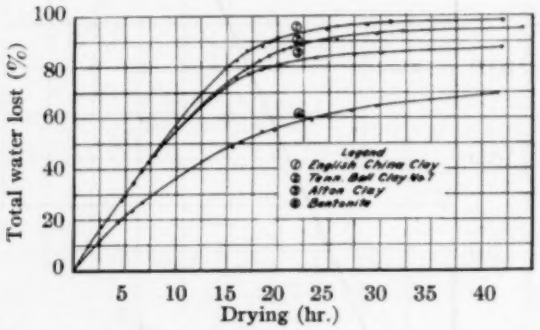

FIG. 9.—Rates of drying of H clays dried in open air at room temperature.

out below. Such clays could never be made single-base clays due to the continual solution of this constituent.

A possible method of evaluating the organic matter content of clays would be a determination of its equilibrium moisture in comparison with clays not containing it. An alternative is to be found in heat-of-wetting measurements which show a similar anomaly.

(5) Permeability

The permeability data in Fig. 7 show first of all that there is a general relationship between permeability and base-exchange capacity, but the correlation is not exact. This is the first of the properties discussed which could be related to the packing characteristics of the particles (see outline section I (3), p. 111).

This relation is clearly indicated here from two different aspects. In method (1) (see section II (2), p. 112), the powdered clays are merely allowed to soak overnight, so the permeabilities are partly dependent on the slaking rates of the clays. More thorough agitation reduced the permeabilities, but the values still fell short of the limiting case brought about by complete dispersion (method 3). The correlation for method 3, which approaches limiting dispersion, is very poor. This lack of correlation evidently means that permeability depends not only on base-exchange capacity but on packing as well and that there is no definite relationship between base-exchange capacity and packing. Note that here again the clays con-

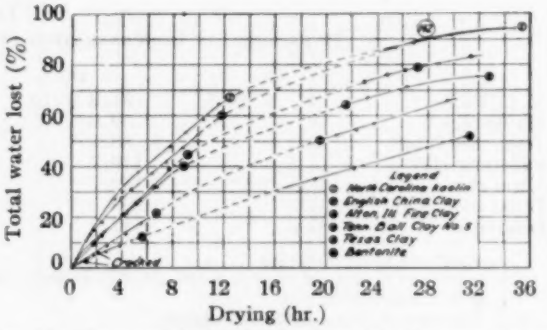

FIG. 10.—Rates of drying of Na clays dried in open air at room temperature.

taining organic matter* do not fall on the curves. This effect could have been predicted from the equilibrium moisture data. The less highly hydrated organic ions can pack much closer and develop a denser structure.

The effect of different cations on the permeability of clays has been shown by Lutz.[18] Some of his data are shown in Fig. 8. The order of increasing permeability is the same as would be expected from a calculation of the field strengths and hydration power for the respective ions (see discussion under Heat of Wetting, section II (2 *B*), p. 112, and Tables I, II, and III).

Information of this sort has several practical applications. The theory can be applied to the modification of drying properties, casting rates, dry strengths, and drilling muds. The data of Fig. 7 offer a partial explanation for some of the frequently observed anomalous behaviors of clays and ceramic mixes in practice. It may be very difficult, if not impossible, always to obtain the same degree of dispersion of the clays during processing, which would have a marked influence on several important properties.

(6) Rate of Drying

Figures 9 and 10 show the results of some simple tests on the rates of drying of several of the clays. The only new facts brought out by these data are the differences in the shapes of the time-water loss curves of the Na and H clays. The H clays dry in the usual characteristic manner, but the curves for the Na clays do not have the shape commonly encountered among water-loss–time curves. The explanation seems to be that the type of packing is so different in the two cases as to alter drastically the structure of the capillary system. The H clays of course are in a flocculent condition, and the floccules of clay pack in a rather loose, unstable structure. As drying progresses and shrinkage takes place, the internal stress is partially relieved by shiftings of the particles composing the floccules. This action not only brings about a more stable and dense packing, but it continually changes the pore

[18] J. F. Lutz, "Physiochemical Properties of Soils Affecting Soil Erosion," *Univ. of Mo. Agric. Expt. Station Research Bull.*, No. 212; 45 pp. (July, 1934).

* Tennessee ball clay No. 5, Alton 5, and peat have base-exchange capacities of 12.1, 21.9, and 76.7, respectively.

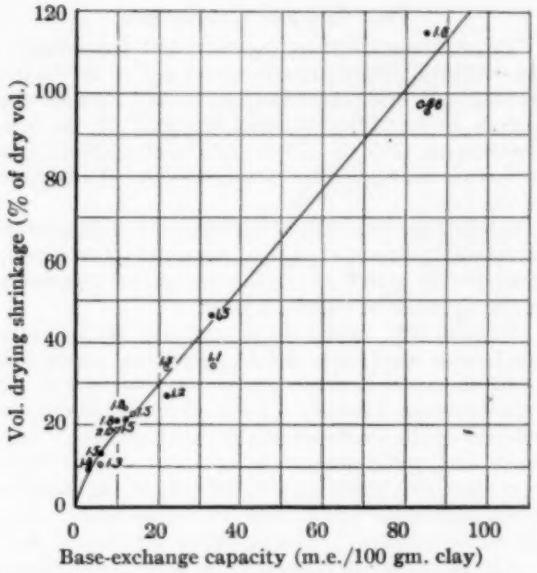

FIG. 11.—Drying shrinkages of clays; numbers near points refer to plasticity of the specimen according to the Endell apparatus; these are all in the stiff-mud range; open circles, H clays; dots, Na clays.

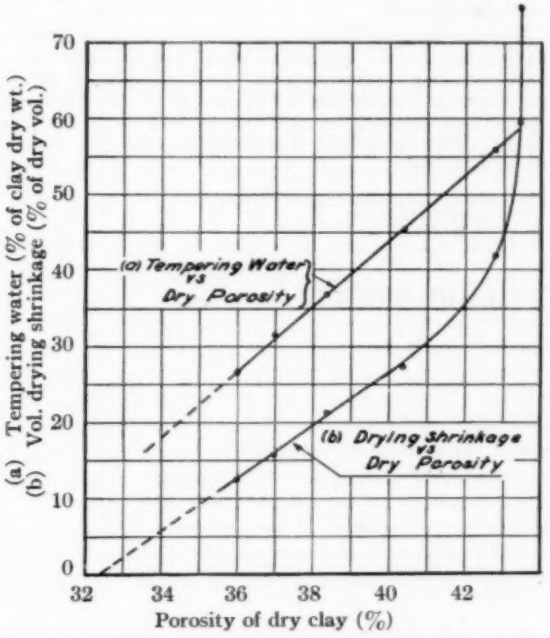
(a) Tempering water (% of clay dry wt.)
(b) Vol. drying shrinkage (% of dry vol.)
(a) Tempering Water vs Dry Porosity
(b) Drying Shrinkage vs Dry Porosity
Porosity of dry clay (%)

FIG. 12.—Effect of tempering water on shrinkage and porosity of Tenn. ball clay No. 7.

structure in such a manner as to contribute toward a continually decreasing rate of drying.

Sodium clays, being deflocculated, are difficult to work unless they possess almost a minimum of water content, which results in a stable system of packing that does not change materially as drying progresses. Clays with such a capillary system should dry with different time-rate curves than do flocculated clays. There is no other means of relieving excess stress

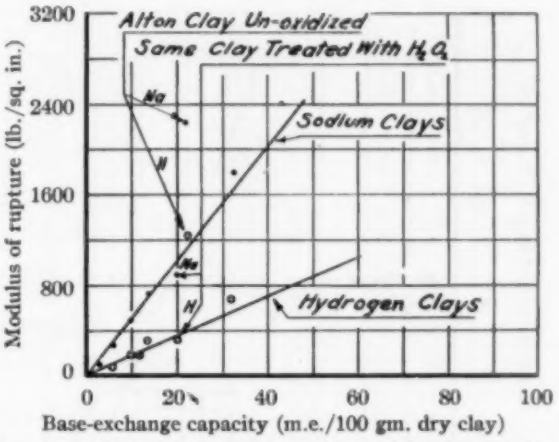

FIG. 13.—Modulus of rupture of Na and H clays in dry state.

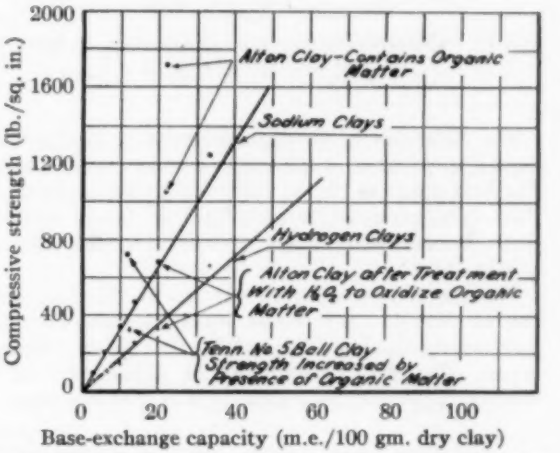
Alton Clay—Contains Organic Matter
Sodium Clays
Hydrogen Clays
Alton Clay after Treatment With H_2O_2 to Oxidize Organic Matter
Tenn. No. 5 Ball Clay Strength Increased by Presence of Organic Matter
Compressive strength (lb./sq. in.)
Base-exchange capacity (m.e./100 gm. dry clay)

FIG. 14.—Compressive strengths of dry clays as function of base-exchange capacity and as influenced by adsorbed Na and H ions and the presence of organic matter.

except to crack. Such clays are difficult to dry safely however, chiefly because of their low permeabilities.

(7) Drying Shrinkage

Figure 11 indicates that if clays are made up to the same plasticity, the drying shrinkage is proportional to the base-exchange capacity, and the effect of the nature of the adsorbed cation is minimized. This is perhaps due to compensating effects of more water and higher porosity in the hydrogen clays and less water and lower porosity in the sodium clays. The relations between drying shrinkage, tempering water, and porosity for a single clay are shown in Fig. 12.

(8) Dry Strengths

Analysis of the dry-strength data shown in Figs. 13 and 14 brings out some interesting points. The same samples that showed poor correlation on the equilibrium moisture and permeability diagrams are also out of place here and in the same direction. Dry strengths are vastly increased by replacing hydrogen with sodium. Organic matter has a similar behavior.

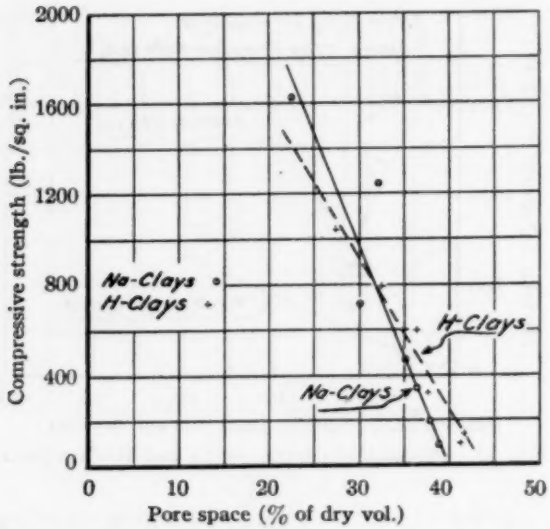

FIG. 15.—Compressive strengths of dry clays as function of their porosities.

The difference in strength is probably due to difference in packing characteristics and pore structure. The data shown in Fig. 15 indicate that this is the case. The clays containing organic matter, which showed poor agreement in Figs. 6, 7, 13, and 14, appear normal in Fig. 15.

The porosity-strength curves for the H clays and the Na clays do not coincide, which indicates that the pore structures of the Na and H clays are of different types. The dry strength would apparently be a function of porosity for a given type of pore structure.

IV. General Conclusions

The cation-adsorption capacity and the nature of the adsorbed cation are closely related to the heat of wetting, pH, and equilibrium moisture. In fact, they appear to be different manifestations of the same phenomena. For a given adsorbed cation, these properties relate directly to the intensity of adsorption of the ion.

It is feasible to postulate the existence of organic ions or ionized groups (originating from the solution of organic matter in clays) to explain the anomalous behavior of clays containing organic matter.

Permeability, drying rates, and dry strengths (for single-base clays) are closely correlated and are dependent on pore structure and pore volume as well as on base-exchange capacity. Pore structure bears some relation to the character of the cation present. Large weak ions, when present, bring about a dense, stable pore structure, which imparts difficult drying characteristics, high dry strength, and low permeability. Small strong ions, such as hydrogen, induce the reverse effects.

The properties of clays may be defined as functions of ion-sorption capacity, nature of the adsorbed cation, and packing, providing the water content and soluble salts are controlled.

Acknowledgment

The authors are indebted to R. H. Bray for his helpful advice and for the use of his laboratory facilities for the base-exchange determinations. J. E. Gieseking, through his generous loan of laboratory facilities and his personal assistance, made possible the pH measurements. The X-ray diffraction work was done through the courtesy of G. L. Clark.

DEPARTMENT OF CERAMIC ENGINEERING
UNIVERSITY OF ILLINOIS
URBANA, ILLINOIS

SPLITTING OF SOFT-MUD BRICK*

BY H. G. SCHURECHT AND J. F. MCMAHON

ABSTRACT

A study was made of the cause and methods of preventing the splitting of Hudson River soft-mud brick. The splitting occurred in the kiln and paralleled the 8- by 4-in. face of the brick and was found to be associated with black coring. Tests made on various portions of the brick showed that the black portions were more vitreous and had lower thermal expansions than the outer, more oxidized portions. On cooling, the stresses resulting from the difference in thermal expansion were such as to tend to split the brick. Modification of brick mixes and method of setting are recommended to overcome black coring.

I. Introduction

Some Hudson River soft-mud brick were found to have cracked and split in a peculiar way. Most of the defective brick showed large cracks that were continuous around the middle and parallel to the 8- by 4-in. faces; many of the brick were actually split in two pieces. The brick were fired in scove kilns, and the faulty brick were found in the twenty-four courses directly above the closing courses on the arch; only a few were in the upper portion of the kiln and none in the arch "legs."

The defective brick had either black or dark brown cores, both of which are due to poor oxidation (Fig. 1). The remedy, as found by this study, was to improve the oxidation.

II. Materials and Methods of Study

The clays, sands, and fuels used were obtained from the plant where these defects were encountered.

Black, brown, and red portions were cut from the

* Presented at the Forty-Sixth Annual Meeting, The American Ceramic Society, Pittsburgh, Pa., April 4, 1944 (Structural Clay Products Division). Received December 21, 1944.

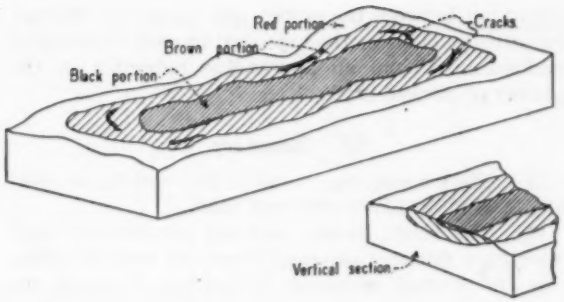

FIG. 1.—Black and brown cores in split soft-mud brick.

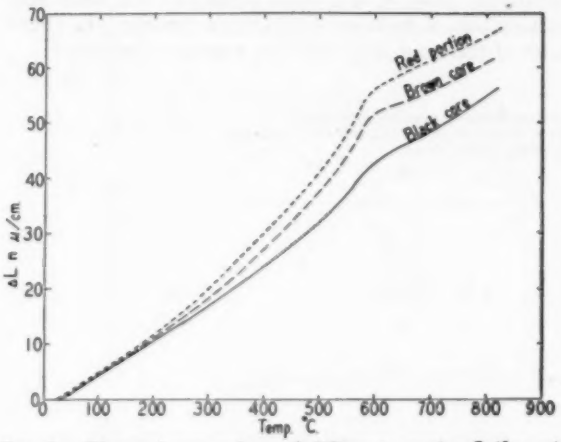

FIG. 2.—Thermal expansions of different portions of cored brick.

split brick and their absorption, density, and thermal expansion were determined (Fig. 2).

To obtain heat distribution in general practice, 2% combustible (coal or coke) is added to the brick mix. In order to determine the relative ease with which these fuels, fine and coarse, could be burned as well as the effect of local clays and sands on the rate of oxidation, the various mixtures shown in Fig. 3 were made up to soft-mud consistency, formed into 2-in. cubes, dried at 100°C., and fired to 600°C. (at 50°C. per hr.). The kiln was held at 600°C. for periods of ½, 1, 2, 4, 6, 8, 10, 12, and 14 hours. Representative samples were then removed, cut through the middle, and examined for the extent of oxidation.

III. Discussion of Results

The differences in thermal expansion between the various portions are considered to be pertinent in relation to cracking and splitting. The outer portion of the brick had the highest thermal expansion, the brown portion an intermediate amount, and the black core the lowest. Because of these differences in thermal expansion, strains developed in the brick.

During cooling, the black core does not contract as much as does the brown portion, which puts the brown core under tension. Because the brown portion contracts less than does the red exterior of the brick, the red portion is also put under tension. Both of

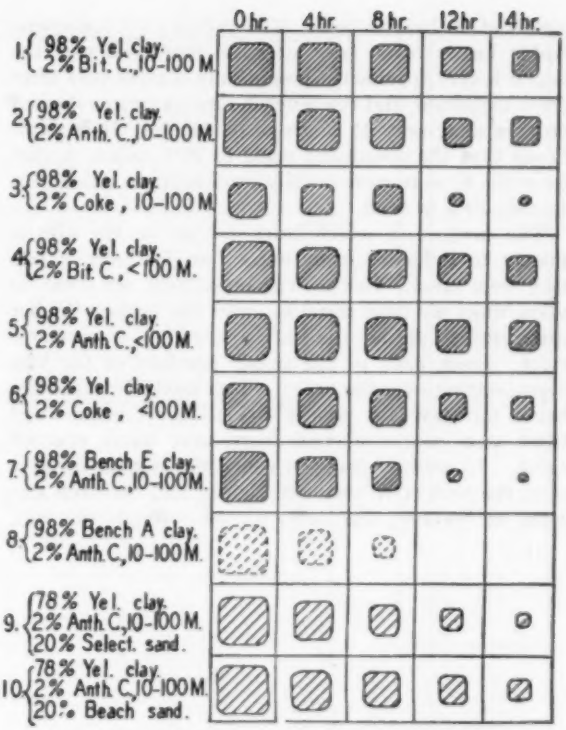
0 hr.
4 hr.
8 hr.
12 hr.
14 hr.
1. 98% Yel. clay, 2% Bit. C., 10–100 M.
2. 98% Yel. clay, 2% Anth. C., 10–100 M.
3. 98% Yel. clay, 2% Coke, 10–100 M.
4. 98% Yel. clay, 2% Bit. C., <100 M.
5. 98% Yel. clay, 2% Anth. C., <100 M.
6. 98% Yel. clay, 2% Coke, <100 M.
7. 98% Bench E clay, 2% Anth. C., 10–100 M.
8. 98% Bench A clay, 2% Anth. C., 10–100 M.
9. 78% Yel. clay, 2% Anth. C., 10–100 M., 20% Select. sand.
10. 78% Yel. clay, 2% Anth. C., 10–100 M., 20% Beach sand.

FIG. 3.—Oxidation of brick mixtures at 600°C.

TABLE I

ABSORPTION AND BULK DENSITY OF PORTIONS OF SPLIT BRICK

	Absorption (%)	Bulk density (gm./cc.)
Black core	8.0	1.87
Brown core	16.0	1.80
Red exterior	26.0	1.60

these strains tend to crack and finally split the brick. Cracking probably starts with the red portion, which is the weakest, and continues through the brown portion, and finally through the black core. The brick oftentimes do not split until they are handled. The fact that the brick usually crack parallel to the 8- by 4-in. face rather than in other directions is accounted for by the lenticular shape of the core, which parallels the 8- by 4-in. face, and by its presence close to or at the surface at the setting points on the 8- by 2-in. face.

To overcome the cracking, it is necessary to prevent coring. The experiments with materials typical of those used along the Hudson River show that their proper selection will assist oxidation. Figure 3 shows coke to be more readily oxidized than either bituminous or anthracite coal and that the oxidation progresses more rapidly when the coarser particles (−10- on 100-mesh) were used.

The addition of the sand greatly facilitated oxidation, but a selected sand (somewhat coarser) was more effective than ordinary beach sand. That oxidation can be promoted by clay selection is indicated by the results obtained with mixes Nos. 2, 7, and 9 (Fig. 3), each containing 98% of clay and 2% (−10- on 100-

mesh) of anthracite coal. The yellow clay specimens had a heavy black core after 14 hours, whereas the bench E clay specimens showed only a small core after the same period, and the bench A clay specimens showed no core after only 12 hours of oxidation. It is significant that the specimens made of 98% bench A clay (mix No. 8) were more readily oxidized than mixes containing 20% of sand.

The manner in which brick are set in the kiln is known to influence oxidation. Two methods of setting were tried. In one, the brick were set so as to allow more air than usual to enter the firebox (higher arch) and to permit the heat to travel in a comparatively direct path to the upper portions of the kiln (open setting over the arch). This method heated the brick too fast for proper oxidation. Carbon-cored brick were numerous and there were many cracked brick. In another firing in which the courses directly over the arch were set more tightly and the arch legs were set loosely, the gases passed through the legs, spread out between the arches, and thence up through the setting. This method resulted in more thoroughly oxidized brick and an appreciable reduction in the number of cracked brick.

IV. Summary

(1) Black coring may result in the cracking or splitting of Hudson River soft-mud brick.

(2) The black, brown, and red portions of cored brick have different physical properties and the differences in thermal expansion are such as to crack the brick.

(3) To lessen the amount of black coring, attention should be given to the clays available, the kind and particle size of fuels incorporated in the mix, the character of the sand used, and the manner of setting.

Ceramic Research Department
New York State College of Ceramics
Alfred, New York

OFFICIAL PERSONNEL OF DIVISIONS, 1944–1945

	Design	Enamel	Glass	Materials and Equipment	Refractories	Structural Clay Products	White Wares
Trustee	W. A. Weldon	R. L. Fellows	J. S. Gregorius	J. E. Eagle	J. B. Austin	Frederick Heath, Jr.	J. W. Hepplewhite
Chairman	W. A. Weldon	H. D. Carter	K. C. Lyon	J. R. Kauffman	W. R. Kerr	R. L. Stone	J. W. Whittemore
Vice-Chairman	Theodore Lenchner	W. W. Higgins	Louis Navias	J. F. Day	S. M. Swain	E. F. Theobald	R. M. Campbell
Secretary	Myrtle M. French	D. G. Moore	S. R. Scholes	V. J. Roehm	E. E. Callinan	R. L. Ferguson	C. M. Lambe, Jr.
Division Nominations	Alice A. Ayars K. E. Smith	F. R. Porter M. J. Bahnsen Karl Kautz	R. A. Miller W. R. Lester L. W. Peterson	J. F. McMahon E. M. Rupp	J. B. Austin C. L. Thompson G. J. Easter	A. P. Potts R. L. Ferguson C. F. Wiseman	J. R. Beam F. C. Henderson R. Russell, Jr.
Papers and Program	C. M. Harder Vincent Broomhall H. L. Moody	W. W. Higgins	Louis Navias	W. E. Dougherty E. W. Emrich J. S. Breitenstein	C. A. Freeman W. S. Debenham B. L. Dorsey	A. C. Jackson H. L. Winburn J. G. Seanor	E. P. McNamara
Membership	W. J. Harr Herbert Tepping G. W. Fichter C. K. Williams	A. I. Andrews J. F. Hunt F. A. Petersen	F. V. Tooley R. R. Shively	E. M. Rupp	L. C. Hewitt F. E. Lobaugh H. M. Parkhurst E. M. Sarraf	C. F. Tefft L. R. Whitaker H. C. Plummer J. H. Isenhour	A. A. Wells
Standards		R. L. Cook W. N. Harrison R. M. King F. A. Petersen B. W. King, Jr.	Members are Comm. C-14, A.S.T.M.	R. C. Meeker	Members are Comm. C-8, A.S.T.M.	G. R. Robinson	F. P. Hall L. E. Thiess
Research		J. C. Reimers	Alexander Silverman O. G. Burch C. E. Leberknight	R. R. Robinson	E. C. Petrie	G. A. Bole H. C. Plummer	R. Russell, Jr. Glenn Howatt
Classification and Nomenclature	Mrs. J. W. Dixon	G. H. McIntyre E. E. Bryant	E. P. McNamara	J. F. McMahon	C. M. Dodd	E. F. Theobald R. E. Grim	A. S. Watts
Rules	J. P. Thorley	W. A. Deringer O. E. Mulvane	S. R. Scholes	Philip Dressler	S. F. Walton	Howells Fréchette	J. D. Clark
Councillors		D. G. Bennett	R. W. Wampler J. F. Greene	V. V. Kelsey		L. R. Whitaker A. P. Potts	
Exhibitions	Mrs. L. S. Backus		J. E. Frazier				
Industrial Management			C. J. Uhrmann	S. S. Cole	J. L. Crawford	J. C. Peck	
Bibliography	P. E. Cox	J. F. Rosenberg		C. L. Cruikshank			

Officers of Classes

	Institute of Ceramic Engineers	Ceramic Educational Council
Trustee	H. M. Kraner	R. M. Campbell
President	M. F. Beecher	C. M. Dodd
Vice-President	T. A. Klinefelter	A. I. Andrews
Secretary	R. S. Bradley	P. S. Dear

THE AMERICAN CERAMIC SOCIETY TRUSTEES AND OFFICERS FOR 1944–1945

President: E. H. Fritz, Stupakoff Ceramic & Mfg. Co., Latrobe, Pa.
Vice-President: C. Forrest Tefft, The Claycraft Co., Columbus 16, Ohio
Treasurer: J. D. Sullivan, Battelle Memorial Institute, Columbus 1, Ohio
Secretary-Editor: R. C. Purdy, 2525 North High St., Columbus 2, Ohio
Past-President: C. E. Bales, Ironton Fire Brick Co., Ironton, Ohio
Past-President: L. J. Trostel, General Refractories Co., Baltimore 3, Md.

TRUSTEES FROM INDUSTRIAL DIVISIONS*

Design: W. A. Weldon, Locke Insulator Corp., Baltimore, Md. (1946)
Enamel: R. L. Fellows, Chicago Vitreous Enamel Product Co., Cicero, Ill. (1946)
Glass: J. S. Gregorius, Pittsburgh Plate Glass Co., Pittsburgh 19, Pa. (1947)
Materials and Equipment: J. E. Eagle, 6306 20th Ave., Green Meadows, Hyattsville, Md. (1945)
Refractories: J. B. Austin, U. S. Steel Corp., Kearny, N. J. (1946)
Structural Clay Products: Frederick Heath, Jr., Owens-Corning Fiberglas Corp., Toledo, Ohio (1945)
White Wares: J. W. Hepplewhite, Edwin M. Knowles China Co., Newell, W. Va. (1947)
Institute of Ceramic Engineers: H. M. Kraner, Bethlehem Steel Co., Bethlehem, Pa. (1947)
Ceramic Educational Council: R. M. Campbell, New York State College of Ceramics, Alfred, N. Y. (1947)

* Date of expiration of term of office in parentheses.

DIVISION OFFICERS

Design
Chairman: W. A. Weldon, Locke Insulator Corp., Baltimore, Md.
Secretary: Myrtle M. French, Art Institute of Chicago, Chicago, Ill.

Enamel
Chairman: H. D. Carter, Harshaw Chemical Co., Cleveland 6, Ohio
Secretary: D. G. Moore, National Bureau of Standards, Washington 25, D. C.

Glass
Chairman: K. C. Lyon, Armstrong Cork Co., Millville, N. J.
Secretary: S. R. Scholes, N. Y. State College of Ceramics, Alfred, N. Y.

Materials and Equipment
Chairman: J. R. Kauffman, Allied Engineering Co., Milltown, N. J.
Secretary: V. J. Roehm, Kentucky Clay Mining Co., Alliance, Ohio

Refractories
Chairman: W. R. Kerr, Armstrong Cork Co., Beaver Falls, Pa.
Secretary: E. E. Callinan, Timken Roller Bearing Co., Timken Steel & Tube Div., Canton 6, Ohio

Structural Clay Products
Chairman: R. L. Stone, Univ. of North Carolina, Raleigh Unit, Raleigh, N. C.
Secretary: R. L. Ferguson, 730 Stuart Bldg., Lincoln, Nebr.

White Wares
Chairman: J. W. Whittemore, Virginia Polytechnic Institute, Blacksburg, Va.
Secretary: C. M. Lambe, Jr., U. S. Gypsum Co., Pittsburgh, Pa.

OFFICERS OF THE FELLOWS

Dean: R. B. Sosman, U. S. Steel Corp., Kearny, N. J.
Associate Dean: Howells Fréchette, Bureau of Mines, Ottawa, Ontario, Canada.
Secretary-Treasurer: R. M. King, Ohio State University, Columbus 10, Ohio

INSTITUTE OF CERAMIC ENGINEERS

President: M. F. Beecher, Norton Company, Worcester, Mass.
Vice-President: T. A. Klinefelter, U. S. Bureau of Mines, Tuscaloosa, Ala.
Secretary: R. S. Bradley, A. P. Green Fire Brick Co., Mexico, Mo.

CERAMIC EDUCATIONAL COUNCIL

President. C. M. Dodd, Iowa State College, Ames, Iowa
Vice-President: A. I. Andrews, University of Illinois, Urbana, Ill.
Secretary: Paul S. Dear, Virginia Polytechnic Institute, Blacksburg, Va.

LOCAL SECTIONS

Baltimore-Washington
Chairman: W. R. Lester, Maryland Glass Co., Baltimore 30, Md.
Secretary: C. B. Shelley, General Refractories Co., Baltimore 3, Md.

Central Ohio
Chairman: W. E. Cramer, Industrial Ceramic Products, Inc., Columbus 8, Ohio
Secretary: John Marquis, O.S.U. Engr. Expt. Sta., Columbus 10, Ohio

Chicago
Chairman: Hugo Filippi, Illinois Brick Co., 228 N. LaSalle St., Chicago 1, Ill.
Secretary: J. J. Svec, Industrial Publications, Inc., 59 E. Van Buren St., Chicago 5, Ill.

Michigan
Chairman: J. F. Quirk, A C Spark Plug Co., Flint 2, Mich.
Secretary: W. V. Blake, Macklin Co., Jackson, Mich.

Northern California
President: W. V. Bragdon, California Faience Co., Berkeley, Calif.
Secretary: P. C. Valentine, Del Monte Properties Co., San Francisco 4, Calif.

Northern Ohio Section
Chairman: E. M. Sarraf, Harbison-Walker Refractories Co., Cleveland 13, Ohio
Secretary: S. M. Swain, North American Refractories Co., Cleveland 14, Ohio

Northwestern Ohio
Chairman: A. H. Couch, Libbey-Owens-Ford Glass Co., Rossford, Ohio
Secretary: H. A. McMaster, Libbey-Owens-Ford Glass Co., Toledo, Ohio.

Pacific-Northwest
President: Gordon Adderson, Gladding, McBean & Co., Renton, Wash.
Secretary: K. G. Skinner, Bureau of Mines, Univ. of Washington, Seattle, Wash.

Pittsburgh
Chairman: H. E. Simpson, Mellon Institute, Pittsburgh 13, Pa.
Secretary: H. M. Parkhurst, General Refractories Co., Pittsburgh 22, Pa.

Southern California
Chairman: R. F. Evans, Gladding McBean, & Co. Glendale, Calif.
Secretary: Guy Wurtsbaugh, Pacific Clay Products, Los Angeles 31, Calif.

St. Louis
Chairman: H. H. Hanna, Pittsburgh Plate Glass Co., Crystal City, Mo.
Secretary: J. H. Ivery, Hydraulic Press Brick Co., St. Louis, Mo.

Upstate New York
Chairman: M. H. Berns, Electro Refractories & Alloys Corp., Buffalo 2, N. Y.
Secretary: E. E. Kunzman, Orefraction, Inc., Pittsburgh 8, Pa.